

The Preveli Nappe, Domani Bay to Korifi Mt.



View of the coast road, which runs along the side the Korifi Mountain between Preveli Beach and Agia Fotia. The road cuttings expose the Preveli Nappe, which is one of the Uppermost Nappes found at the south-central part of Crete. A closer look at the rocks reveals phyllite, green schist, limy schists, mafic dikes and metamorphic mafic rocks.

Compiled by George Lindemann, MSc.

Berlin, August 2024

Content

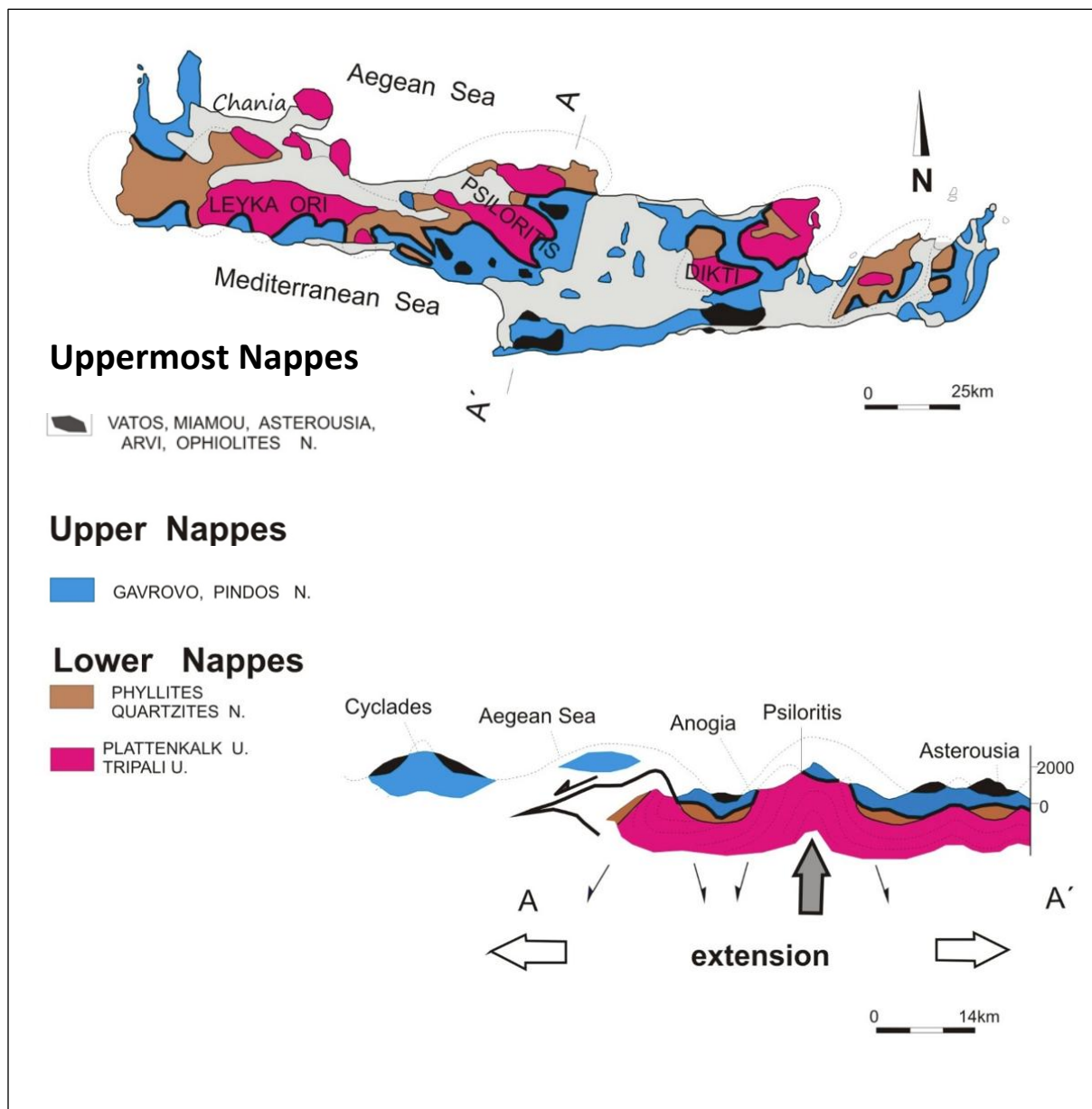
| | | |
|-------|---|----|
| 1 | Introduction..... | 4 |
| 1.1 | Apatite fission-track ages | 6 |
| 2 | Preveli Nappe..... | 7 |
| 2.1 | Main Road to Preveli..... | 11 |
| 2.2 | Venetian Bridge..... | 12 |
| 2.2.1 | Blueschist (Glaucophane and Crossite)..... | 13 |
| 2.3 | Road north of Gianniou | 14 |
| 2.4 | Road south of Gianniou..... | 19 |
| 2.5 | Catsogridio valley, near Preveli | 22 |
| 2.5.1 | Quartz veins and kink bands..... | 25 |
| 2.5.2 | Thrust Breccia | 37 |
| 2.5.3 | Pseudotachylite..... | 39 |
| 2.6 | General Model..... | 41 |
| 2.7 | The Underlying Pindos Unit and Preveli Beach..... | 42 |
| 2.8 | Coast Road | 45 |
| 3 | Appendix..... | 63 |

Appendix

| | |
|---|----|
| Geological Time Scale | 63 |
| Geological Map of the Uppermost Nappes near Plakias by Krahle, 1981 | 64 |
| Plate Tectonic Model for the Uppermost Nappes by Tortorici, 2011 | 65 |
| DA Event..... | 66 |
| DB Event..... | 66 |
| DC Event..... | 66 |
| DD Event..... | 66 |
| Conclusions | 66 |
| Fission track dating | 67 |
| Applications..... | 67 |
| Provenance analysis of detrital grains | 68 |
| Metamorphic Facies | 69 |
| Metamorphosed Pelitic Rocks (Metapelites)..... | 71 |
| Slate | 71 |
| Phyllite..... | 71 |

| | |
|---|----|
| Schist | 71 |
| Gneiss | 72 |
| Minerals in Metapelites | 73 |
| Metamorphosed Limestones and Dolostones (Marbles) | 75 |
| Metamorphosed Mafic Rocks (Metabasites) | 76 |
| High-Pressure Rocks and Minerals | 80 |

1 Introduction



Journal of the virtual explorer _NW Crete_online

The Preveli nappe, also regarded by some as part of the Vatos nappe (Bonneau and Lys, 1978; Bonneau, 1984), forms one of the subunits of the Uppermost Nappes. The subunits underwent metamorphism and exhumation at different times in the Mesozoic, independently from each other (Tortorici et al., 2012). From the early Cenozoic onwards, the Uppermost units are considered to have been part of the upper crust of the Eurasian active continental margin (Thomson et al., 1998). Owing to the Miocene collision with the Adriatic microcontinent, the

upper crust of the active margin was emplaced on top of the nappe pile that was stacked as a result of the northward directed subduction of the Pindos Ocean (Hall et al., 1984; Robertson et al., 1991; Fassoulas et al., 1994; Jolivet et al., 1994; Thomson et al., 1999). On Crete, remnants of the Uppermost Tectonic Unit are locally preserved in graben structures. [Source: J. Nüchter, 2013]

The Preveli nappe consists of Permian meta-siliciclastic rocks covered by limy phyllite and middle to late Permian limestone (now marble) (Bonneau and Lys 1978), and bimodal metavolcanic rocks. The metavolcanic rocks developed in a Triassic extensional setting and led to the formation of skarn (Zulauf et al. 2023a). Towards the stratigraphic top, the mafic metavolcanic rocks dominate and are related to Upper Triassic to Jurassic (meta)chert and cherty marble (Krahl et al. 1982). The Preveli rocks underwent Eohellenic deformation under epidote-blueschist-facies conditions at $T = \text{ca. } 370^\circ\text{C}$ (Koepke et al. 1997; Tortorici et al. 2012; Zulauf et al. 2023b). The main tectonic transport during late nappe emplacement was top-to-the west. [Zulauf G. et al., 2023]

The following table shows metamorphic ages based on radiometric dating using either U-Pb or K-Ar isotopes. The data indicates metamorphism of the Preveli and Vatos nappes to have taken place during the Lower Cretaceous and Upper Cretaceous respectively. The age of the original sediments (i.e. protolith age) are significantly different. The Preveli nappe is thought to be of Late Permian - Upper Triassic age, while the Vatos nappe is of Late Jurassic - Upper Cretaceous age.

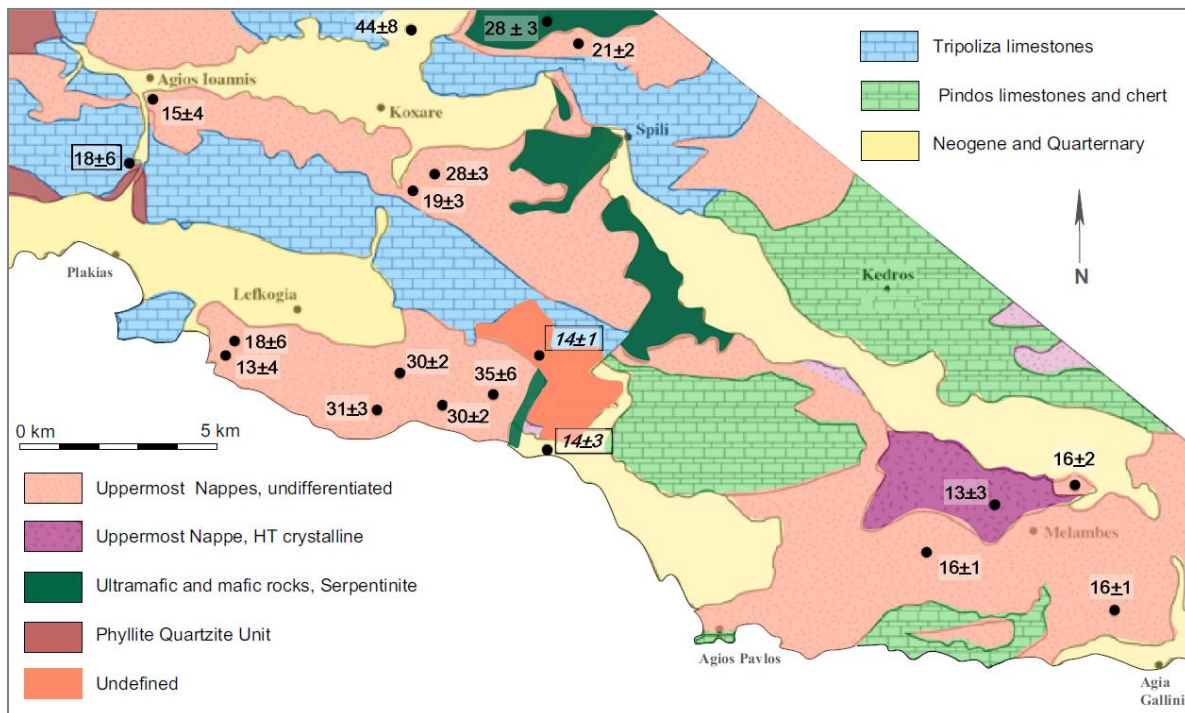
-Table: Radiometric dating of the Vatos and Preveli Nappes within the Uppermost Unit (Zulauf et. al, 2023)

| Unit/nappe Type | Protolith age | Metamorphism | Metamorphism Age |
|-----------------|---|-----------------------------|-----------------------|
| Vatos | Latest Jurassic - Upper Cretaceous (10, 11) | Greenschist (10, 18) | Upper Cretaceous (10) |
| Preveli | Late Permian - Upper Triassic (7, 8) | Epidote-Blueschist (12, 13) | Lower Cretaceous (14) |

(10) Malten (2019), (11) Koepke (1986), (12) Koepke et al. (1997), (13) Tortorici et al. (2012), (14) Zulauf et al. in prep., (18) Karakitzios (1988)

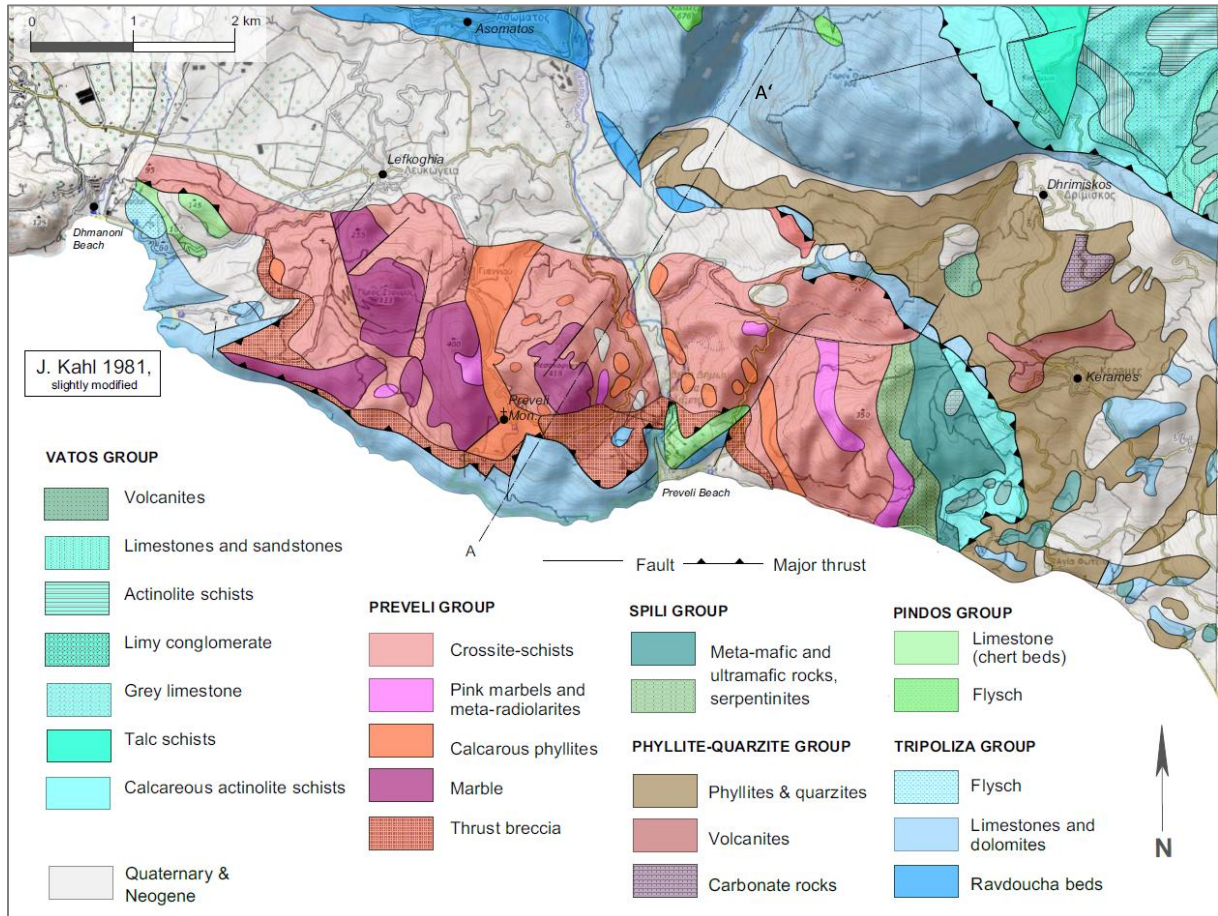
1.1 Apatite fission-track ages

The following Figure shows apatite fission-track results gained from the Uppermost nappes in the Plakias area of southern Crete undertaken by (Thomson, 1999). Fission tracks are preserved in a crystal when the ambient temperature of the rock falls below the annealing temperature, which is between 70 and 110 °C for Apatite (see Appendix for explanation of apatite fission-track ages). The data appears to indicate two periods of cooling one at about 30-35 Ma and another younger one at 13-20 Ma. According to Thomson, 1999 the results require a period of rapid cooling at about 40 Ma ago. This may be related to the very early stages of collision of the leading edge of the Adria Microcontinent with Eurasia. The Uppermost unit rocks must then have remained within similar levels of the crust, some within the apatite partial annealing zone between approx. 120°C and 60°C, until a second stage of cooling at about 16 Ma, when all of the samples of the Uppermost unit cooled to below c. 60°C, where they remained until the present day.



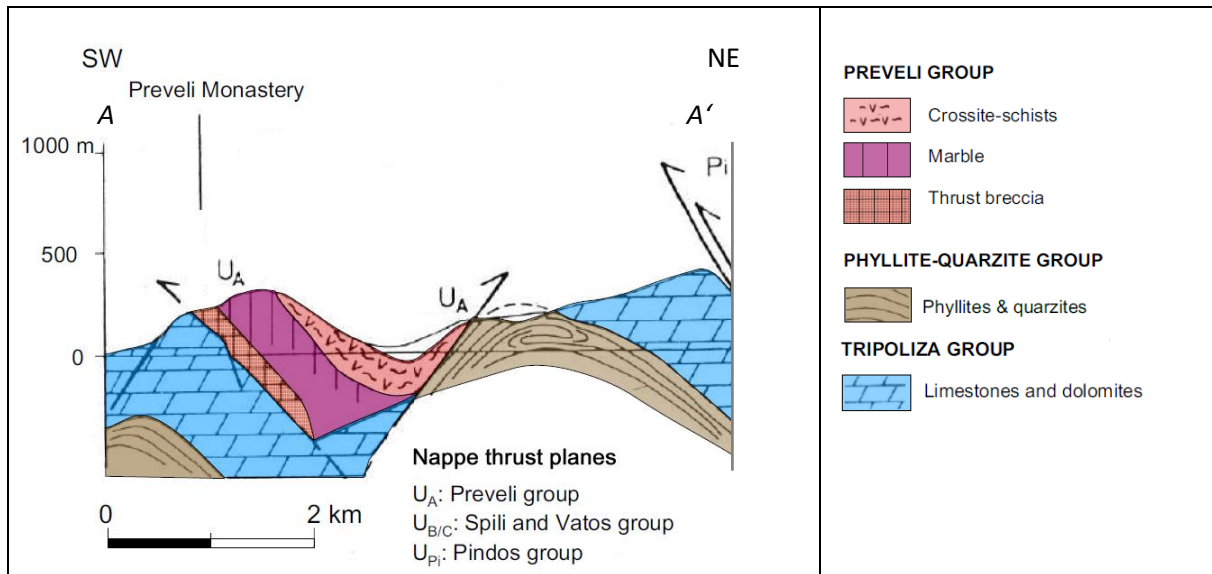
*Fig.3 Geological map of the Plakias area of southern Crete showing **apatite fission-track ages** for the Uppermost nappes (upper plate). Also shown are two ages from the Phyllite-Quartzite unit of the lower nappes (lower plate) [*14 ± 3 ma*] and one age from the Tripoliza unit (upper plate) [*18± ma*] [Thomson, 1999, slightly modified]*

2 Preveli Nappe



After: Krahle, 1981

By means of geological mapping in the area of Damnioni to Kerames the extent of the Preveli Nappe has been determined by Krahle, 1981. Within the mapped area the lithology is characterized by blue-schists indicating LT/HP metamorphism. The Preveli group is divided into six lithological members (Krahle 1981).



Simplified cross section of the Preveli Nappe near the Preveli Monastery. [Source: Krahel S., 1979]

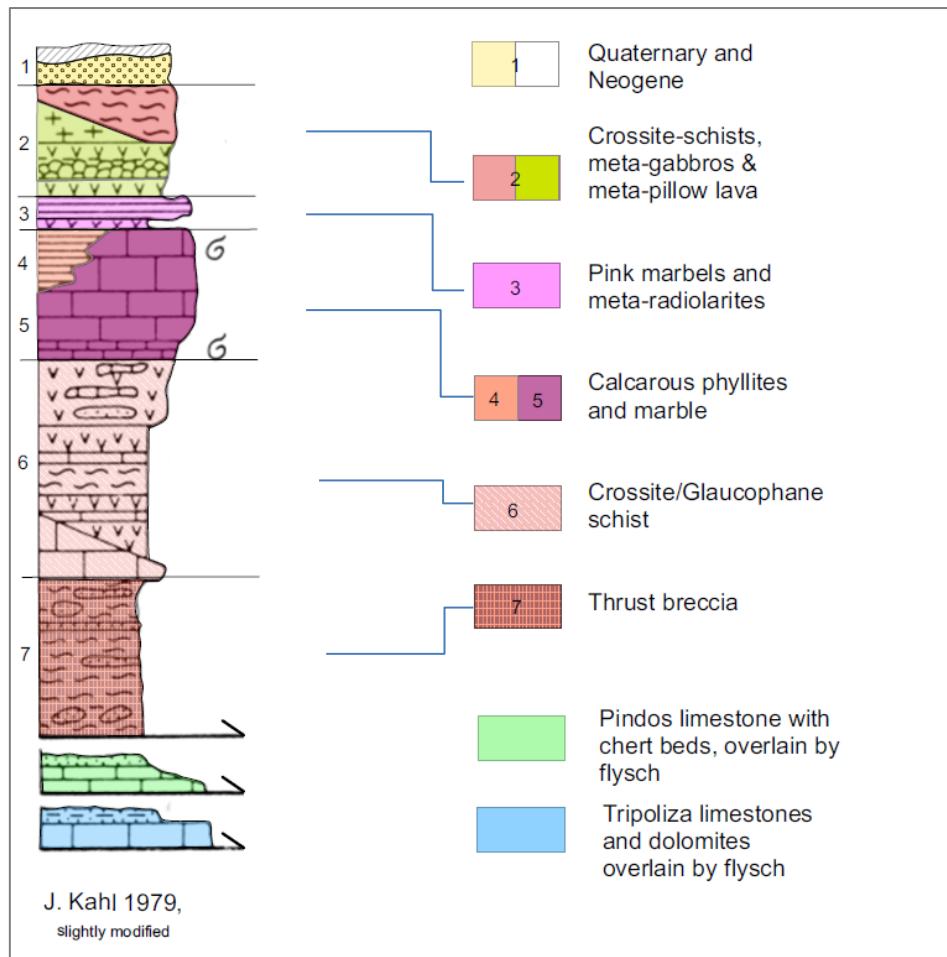



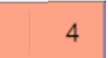

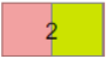
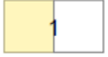
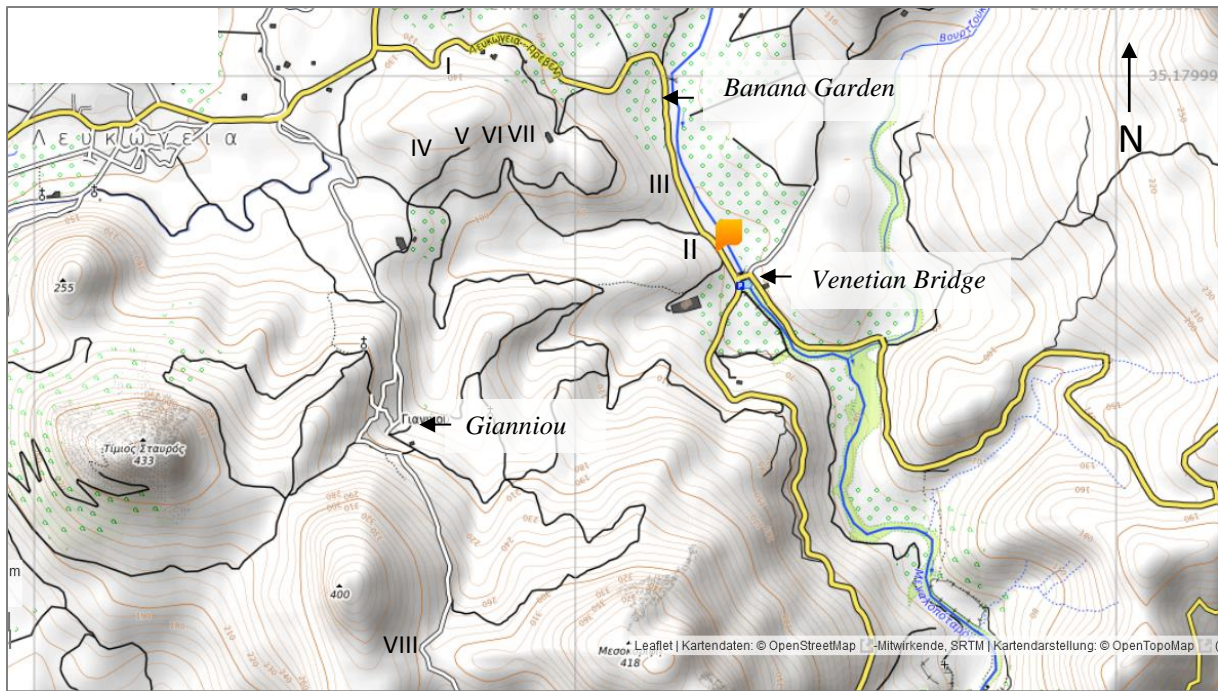


Fig. 2: Lithostratigraphic column of the Preveli Group after Krahle, 1979

| Description of the Preveli Group (Kahle 1979) | |
|--|---|
|  <p>Thrust breccia</p> | <p>The base of the member is formed by a polymict thrust breccia. It is composed of angular clasts of different origin intermixed in a consolidated matrix. It crops out along the south-coast between Damnoni in the west and a small mountain Korifi east of the Amudi creek valley. It lies either on rocks of the Pindos group or of the Tripolitza group.</p> |
|  <p>Glaucophane / crossite schist</p> | <p>Overlying the thrust breccia west of the Amudi creek valley there are sheet-like glaucophane-bearing metavolcanites. In the area east of Damnoni this member is characterized by intercalated meta-sediments of Permian age.</p> |
|  <p>Massive marble</p> | <p>The mapped marbles are fossiliferous. Basic descriptions of the fossil content were given by Bonneau & Lys, 1978 from outcrops east of the Amudi creek valley. North and about 1.5 km west of Preveli Monastery the marble is also fossiliferous.</p> |
|  <p>Calcareous phyllites</p> | <p>The next member upwards consists of thin bedded meta-lime-, silt-, and sandstones. They also yield fossils probably of Permian age. Possibly this member interfingers laterally with the underlying massive marbles of Permian age.</p> |
|  <p>Meta-radiolarites</p> | <p>Overlying the calcareous phyllites there is a group of pink marbles, meta-radiolarites, and meta-volcanites. Neither the marbles nor the radiolarites could be dated. These rocks crop out in numerous fragments east and north-west of the Amudi creek valley and north-east and north-west of the Monastery Preveli</p> |
|  <p>Crossite-chlorite schists</p> | <p>Associated or mostly above the meta-radiolarites there are meta-volcanites with intercalations of meta-clastics. The meta-volcanites display a pillow-lava structure (about 1 km ENE of the monastery). Pebbles of gabbroic rocks may also be observed. Of importance are the intercalated crossite-bearing schists. The crossite-bearing schists' tectonic position is not yet quite clear. Perhaps part of the mapped crossite-schists belong to the basal part.</p> |
|  | <p>Neogene and Quaternary</p> |

Legend to cross section

According to Krahle, 1981 the Preveli group seems not to belong to the basal part of the Uppermost nappes (also known as ophiolitic mélange) as there are rocks of the Spili- and the Vatos group within the basal thrust breccia. Thus, the Preveli group appears to represent a part of a nappe which has been thrust over all other groups. However, Zulauf et. al, 2023 places the Preveli Nappe at the bottom of the Uppermost Unit, as it occurs in contact with the lower lying Pindos unit.



Location of outcrops



Location of outcrops, Sections 2.1, 2.2 and 2.3

2.1 Main Road to Preveli



Outcrop I. Greenstone



Outcrop I. Closeup of the greenstone sample

2.2 Venetian Bridge



Outcrop II. Greenschist outcropping approx. 60m north of outcrop III



Outcrop III. View of the road to the venetian bridge looking south as seen from the blue schist outcrop.

North of Kato Moni Preveli near the venetian bridge on the right side of the road there is an outcrop of blueschist (blueschist facies) with large blue amphiboles visible to the naked eye (N 35° 10.48; E 24° 27.91) [Kull].

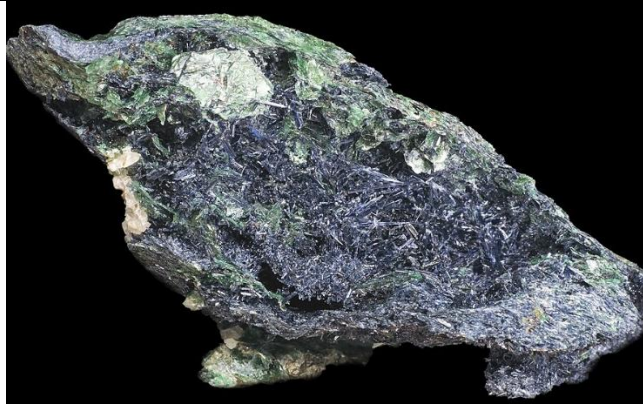


Outcrop III. Blue schist containing glaucophane or crossite

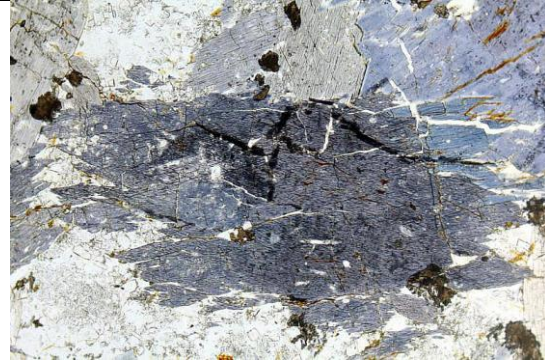
2.2.1 Blueschist (Glaucophane and Crossite)

Glaucophane is the name of a mineral and a mineral group belonging to the sodic amphibole supergroup of the double chain inosilicates, with the chemical formula $\text{Na}_2(\text{Mg}_3\text{Al}_2)\text{Si}_8\text{O}_{22}(\text{OH})_2$. “Blueschist”, gets its name from the glaucophane series, which consists of blue minerals. Glaucophane, along with the closely related mineral riebeckite, to which it forms a series, are the only well-known amphiboles that are commonly blue. Glaucophane, which is the magnesium-rich endmember, forms a solid solution series with ferroglaucophane ($\text{Na}_2(\text{Fe,Mg})_3\text{Al}_2\text{Si}_8\text{O}_{22}(\text{OH})_2$). The two endmembers are indistinguishable in hand specimens. As is the intermediate member in called crossite. Glaucophane's hardness is 5–6 on the Mohs scale.

Glaucophane generally forms in blueschist metamorphic rocks of gabbroic or basaltic composition that are rich in sodium and have experienced low temperature-high pressure metamorphism such as would occur along a subduction zone.



Glaucophane with fuchsite [Wikiwand:
<https://www.wikiwand.com/en/articles/Glaucophane>]



Microscopic image of glaucophane crystals, Milos (Greece). PPL image, 2x (Field of view = 7mm)
<https://www.alexstrekeisen.it/english/meta/glaucophane.php>

Crossite

Crossite belongs to the group of sodium amphiboles, within which it occupies an intermediate position within the glaucophane - riebeckite series and has the chemical formula $\text{Na}_2(\text{Mg,Fe})_3(\text{Al,Fe})_2\text{Si}_8\text{O}_{22}(\text{OH})_2$. It is an amphibole that occurs in regional metamorphic (green schist facies, LT/LP) as well as in low temperature high pressure metamorphic (blue schist facies, LT/HP) rocks. Its crystals are often indistinct, and rarely constitute elongated prisms ; generally, crossite forms lamellar, fibrous, granular or bacillary masses, grey to greyish blue in colour.

2.3 Road north of Gianniou





Outcrop IV. Mica schist



Outcrop IV. 1: Schist containing mica and quartz



Outcrop V. Schist



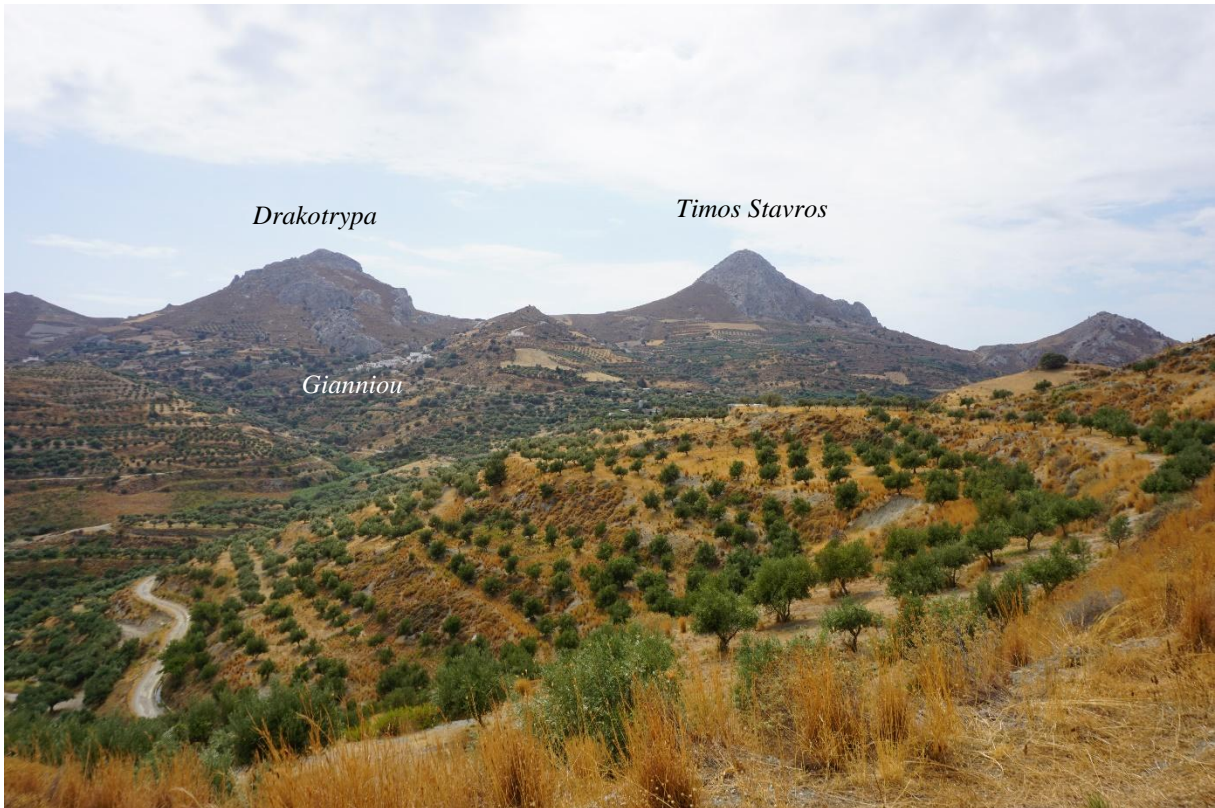
Outcrop V. Closeup of previous picture. Schist containing mainly felsic minerals



Outcrop VI. Schist



Outcrop VI. Closeup of previous picture. Schist



Outcrop VII. View of the village Gianniou and Timos Stavros looking West



Outcrop VII. Folded schist containing mainly mica and quartz

2.4 Road south of Gianniou



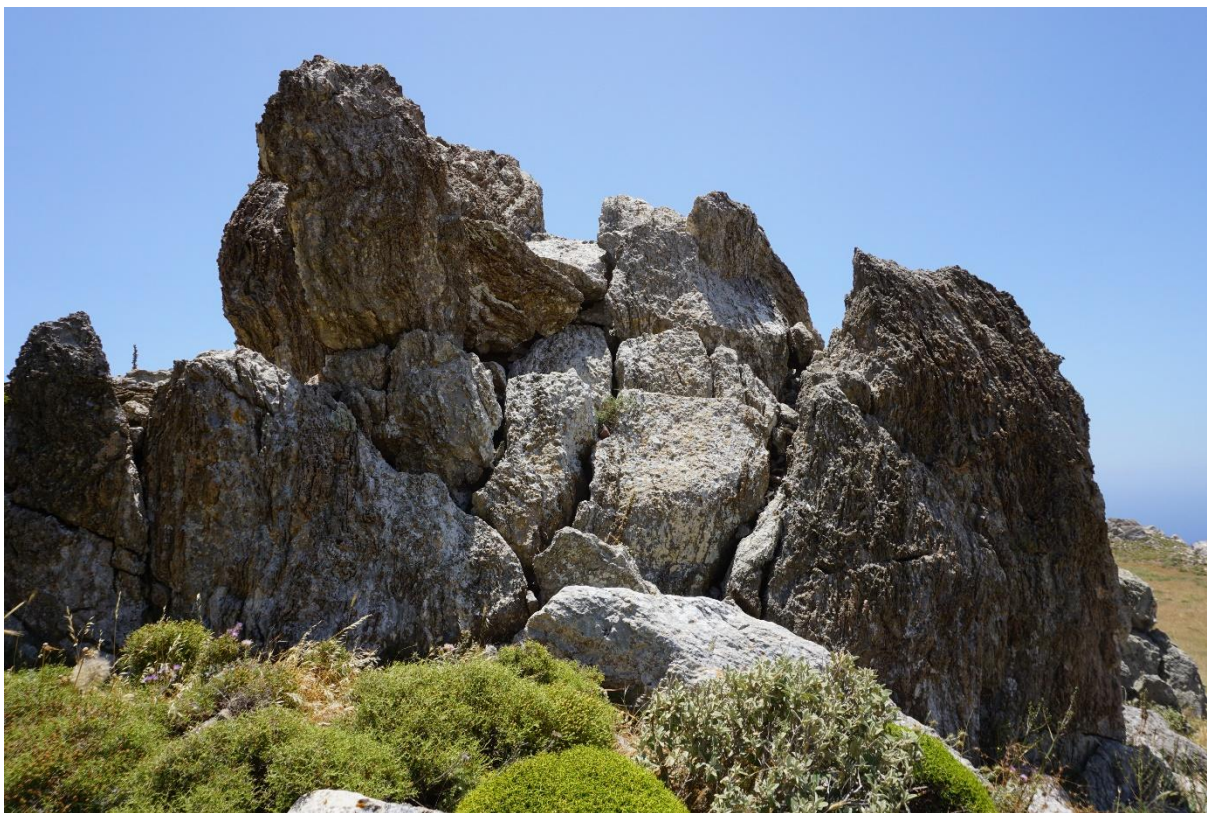
View of Timos Stavros (chapel), Domani and Plakias bay looking westwards from the outcrop



Outcrop VIII. Mica schist



Outcrop VIII. Mica schist



Outcrop VIII.

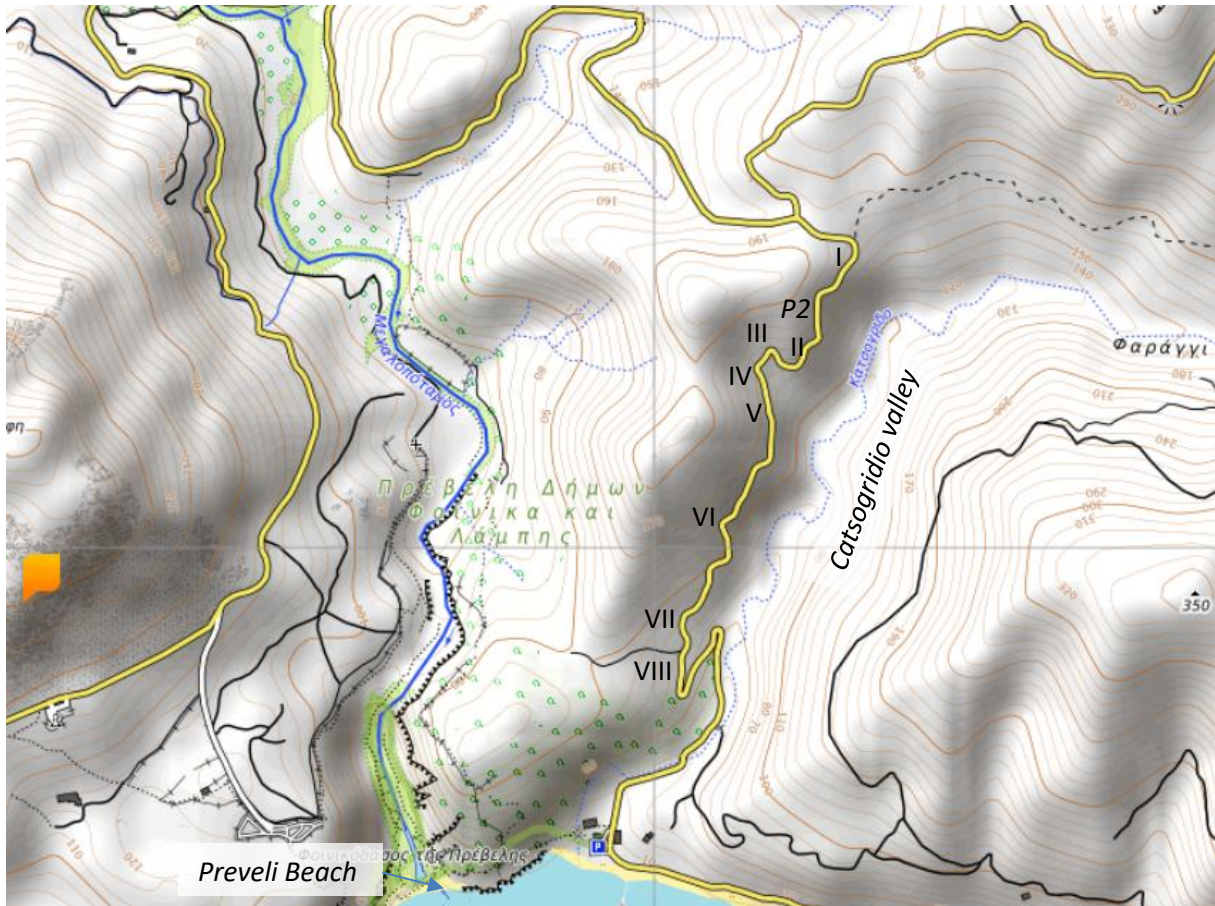


Outcrop VIII. Pink marble and meta-radiolarite ?

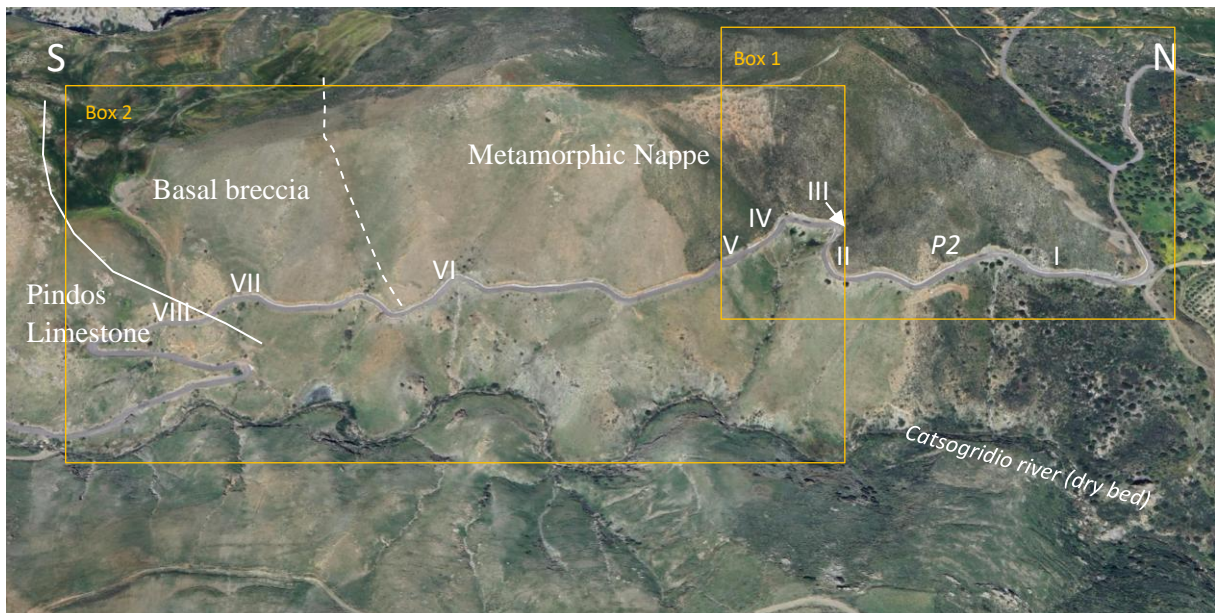


Outcrop VIII. Closeup of sample from same location

2.5 Catsgridio valley, near Preveli



Location of Outcrops within the Catsgridio valley



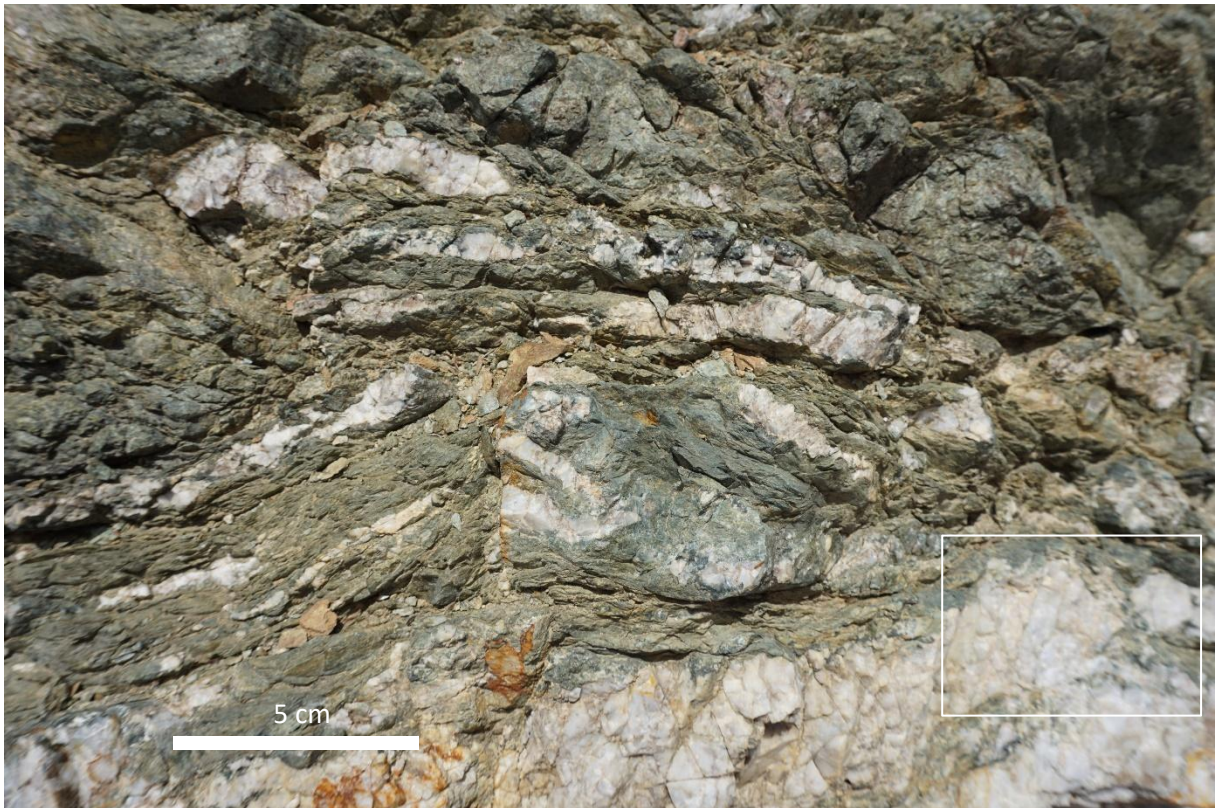
Location of outcrops Catsgridio valley

By studying the base of the Preveli nappe, which now rests on limestone formations, Nüchter, 2013 developed a model describing the thrust fault propagation. The nappe comprises phyllites, quartzites, marbles, metabasites, and metarhyolites, which underwent high pressure-low temperature (HP-LT) metamorphism during the Jurassic [Seidel et al., 1977]. As a result of

intensive deformation the Preveli Nappe displays pervasive schistosity and folds. Koepke et al., 1997 derived peak metamorphic conditions of approximately 0.8 ± 0.1 GPa at $370 \pm 30^\circ\text{C}$. Resting on top of the cherty limestones of the Pindos Unit the Preveli nappe it is well exposed in the Plakias half graben between Kerames Village and the Preveli monastery. Owing to block rotation associated with the formation of the graben, the basal thrust plane dips gently (ca. 10°) toward NE. At the base of the Preveli nappe there is an approx. 30 m thick layer of tectonic breccia. The underlying sedimentary rocks of the Pindos unit show no signs of brecciation [J. Nüchter et. al. , 2013].



Box 1: Location of Outcrops (sample location P2 of Nüchter, et. al., 2013)

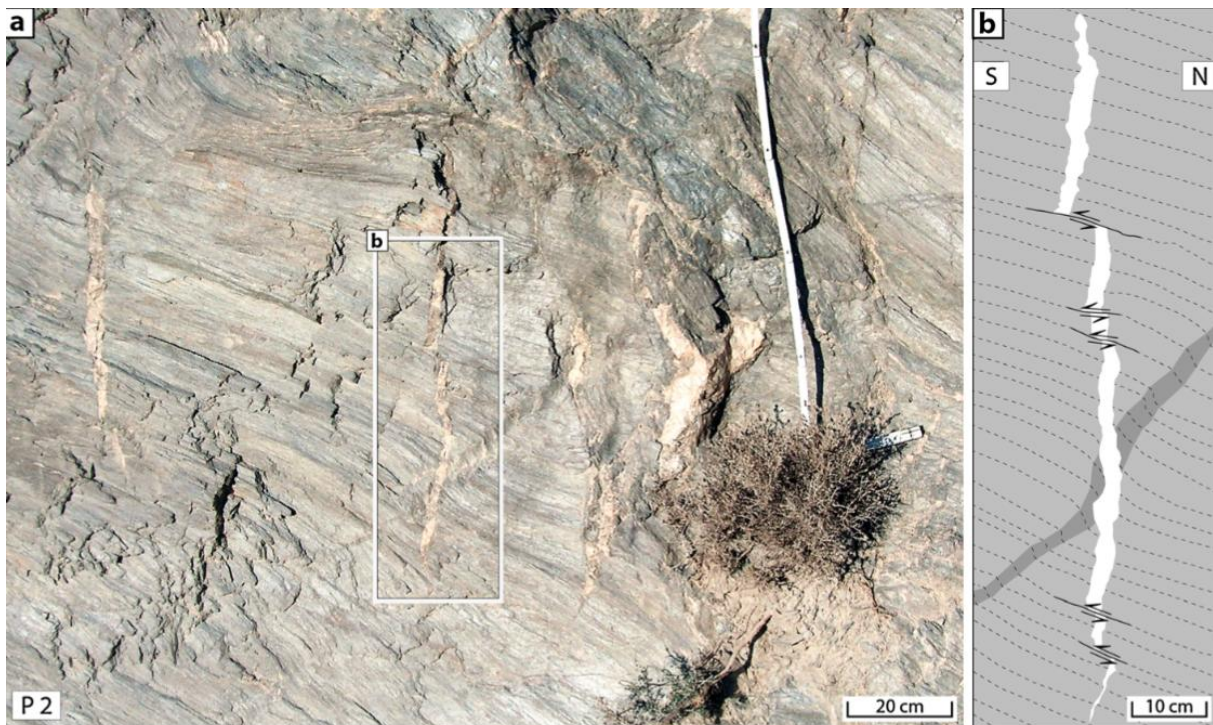


Outcrop I Metamorphic Nappe. Folded quartz vein in green schist



Outcrop I. Closeup of previous picture showing typical glassy lustre of quartz

2.5.1 Quartz veins and kink bands



Outcrop P2; (a) Quartz veins with low aspect ratio discordant to the pervasive schistosity. (b) Quartz vein crosscutting kink band. Sketch showing quartz vein crosscutting kink band and minor shear zones displacing vein parallel to foliation in host rock. [Source: J. Nüchter, 2013]

Kink bands in the Preveli nappe are interpreted to reflect a short episode of plastic deformation. The kink bands along with other earlier structures, such as schistosity and folds are cut by quartz veins. Crosscutting relations indicate that the path of the crack containing the quartz filling shown in the above figure was not affected by pre-existing structural anisotropy but was entirely controlled by the existing tectonic stresses at that time. The microstructure of the sealing quartz indicates that fractures must have widened into open fissures, which were subsequently filled with fluid enabling unconstrained crystallization. Small shear zones off-setting the quartz veins by up to a few centimetres, indicate a stage of deformation after sealing. [Source: J. Nüchter, 2013]



Outcrop I. 1: Greenschist, 2: Calcsilicate schist



Outcrop I; closeup of previous picture (see box): 1: Greenschist, 2: Calcite vein



Outcrop I; Greenschist. Calcite vein indicates post brittle extensional stress after the main ductile metamorphic event. Minor shear stresses parallel to foliation in the host rock have off-set the calcite vein at a later stage.



Outcrop I; Carbonate-silicate schist: 1: Calcite



Outcrop II: Highly deformed schist. At this location the hinges of folds are well exposed. Folding is reported to have taken place at an earlier phase during the Mesozoic.



Outcrop II, closeup of previous picture: 1: Schist, 2: hinge area of a small fold



Outcrop II, closeup of previous picture: 1: calcite vein diagonal to the fold axis indicating brittle extensional stress after the earlier phase of ductile folding.



Outcrop III: Carbonate-silicate schist



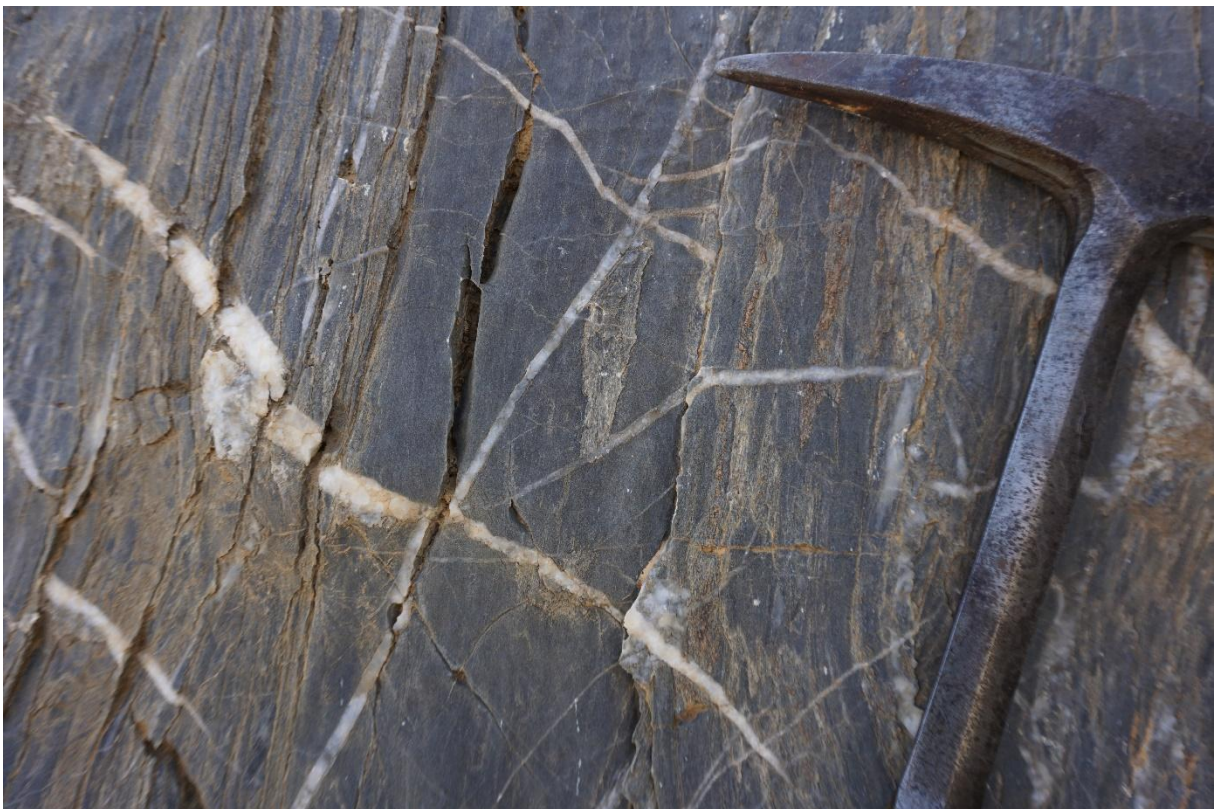
Outcrop III, closeup of previous picture. Carbonate-silicate schist: 1: calcite layer



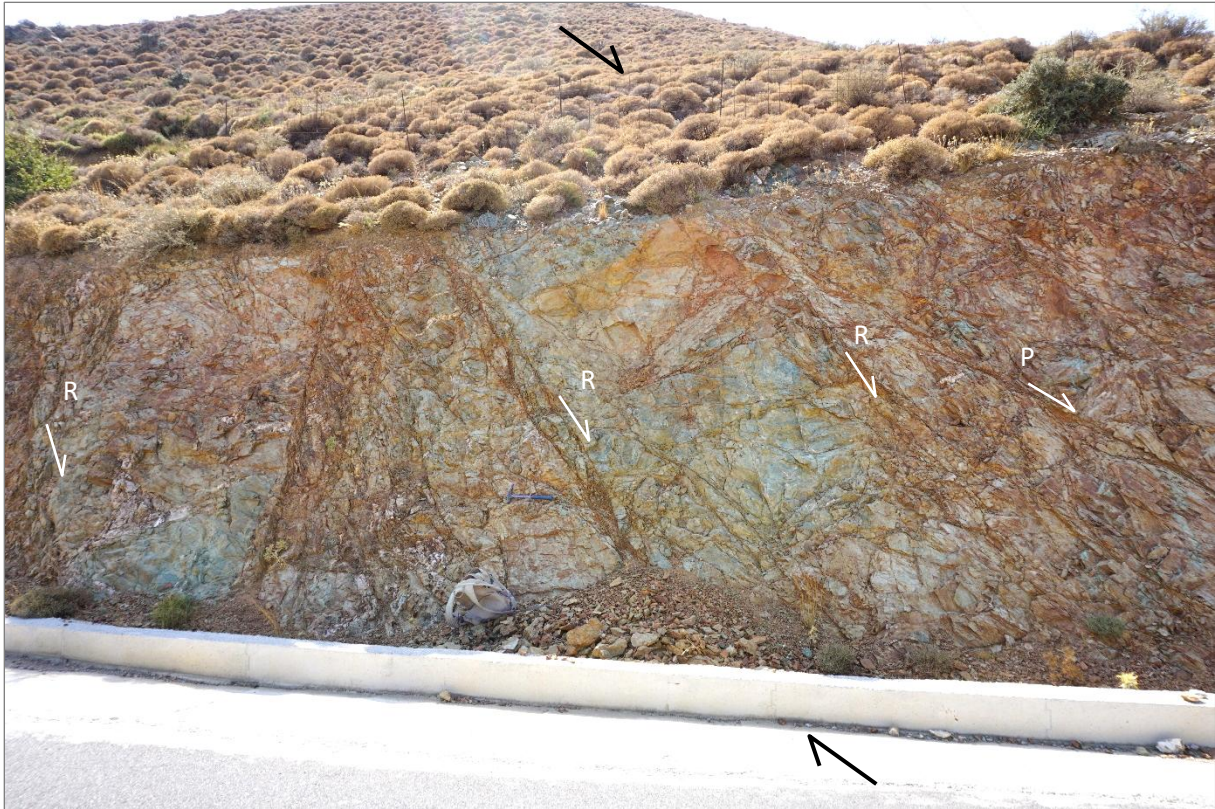
Box 2: Location of outcrops



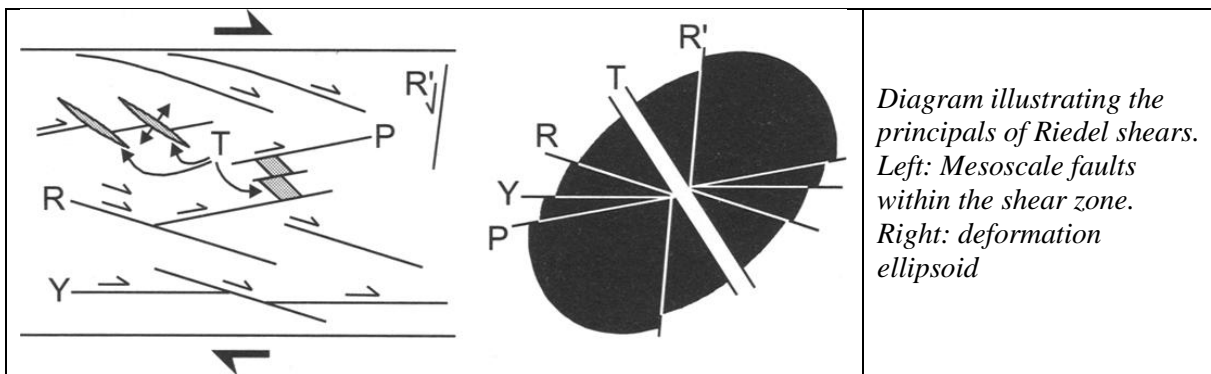
Outcrop IV: Schistose impure marble (calcschist)



Outcrop IV, closeup of previous picture: Schistose impure marble (calcschist)



Outcrop IV: Greenschist displaying a number of faults. These are thought to originate from the Miocene indicating a late stage of brittle deformation due to shear stresses. The faults could well be Riedel shears that are small gently inclined faults indicating movement in the same direction of the main shear plane.





Outcrop V Closeup of previous picture



Outcrop V: 1: possible small-scale shear zones diagonal to foliation. The intensive green colour indicates mafic composition of the rock, which was probably once a basalt or gabbro.



Outcrop VI. System of faults and shear zone indicating a phase of brittle deformation within the metamorphic nappe. The faults that are thought to have occurred during Miocene deformation bear resemblance to Riedle-shears. I: Possible reactivated earlier shear zone.



Outcrop VI: Same outcrop as above seen from a different angle



Outcrop VI: A shear zone and sigmoid structure indicate rough top-to-south direction of movement during an earlier phase of deformation. 1: shear zone; 2: sigmoid structure



Outcrop VI: A different perspective of the shear zone



Outcrop VI: Highly sheared and folded carbonate-silicate schist. White layers of calcite or quartzite in meta-argillaceous rock.



*Outcrop VI: Closeup from the same outcrop showing highly sheared schist reminiscent of a tectonic *mélange*. The light fragments were former calcite or quartzite layers in an argillaceous rock.*

2.5.2 Thrust Breccia

The tectonic breccia was formed at the base of the nappe due to friction as it travelled along its thrust plane. Thick fault breccias are commonly interpreted to develop by incremental sidewall abrasion related to consecutive earthquakes. [Nüchter, 2013]

The breccia clasts came exclusively from the metamorphic rocks and quartz veins of the Preveli nappe, and appear to have no pattern of orientation. Note that Krahle, 1981 has pointed out that the thrust breccia elsewhere contains ophiolite particles and clasts from the Vatos nappes. The breccia at this location is matrix supported and quite hard. Due to the lack of any obvious correlation between the type of clasts, significant travel and rotation must have taken place. All structures inside the clasts formed prior to brecciation. The diameter of the clasts ranges from 10 μm to 10 cm. In the finest fraction, sheet silicates such as phengite and chlorite appear to be enriched relative to other constituents. Enrichment of phengite in the finest fraction is attributed to preferred chipping from phyllites and mica schists (Spray, 1992). Similar clast shapes and size distributions prevail throughout the entire breccia, irrespective of position with respect to the thrust fault. [Nüchter, 2013]



Outcrop VII: Tectonic breccia within the thrust plane below the Preveli Nappe (basal breccial layer).



Outcrop VII: Basal breccial layer of the Preveli Nappe. Solid breccia composed of centimetre-sized fragments embedded in a fine-grained matrix.



Outcrop VII: The clasts of different composition are reported to be solely from the nappe itself



Outcrop VII. Tectonic breccia with centimetre to decimetre-sized fragments that are angular to subrounded (fly middle left of picture for scale)

2.5.3 Pseudotachylyte



Outcrop VII, 1: Tectonic breccia, 2: Pseudotachylyte vein injected into the breccia.



Outcrop VII, 1: Tectonic breccia, 2: Pseudotachylyte vein injected into the breccia. The veins are undeformed.

Pseudotachylyte or Pseudotachylite is a cohesive glassy or very fine-grained rock that occurs as veins and often contains inclusions of wall-rock fragments. Pseudotachylyte is typically dark in colour; and is glassy in appearance. It was named after its appearance resembling the basaltic glass, tachylyte. Typically, the glass is completely devitrified into very fine-grained material with radial and concentric clusters of crystals. In the case of frictional melting at seismic faults it is found either along fault surfaces, as the matrix to a fault breccia, or as veins injected into the walls of the fault (injection vein type). [Source Wikipedia].

At this location the pseudotachylyte veins transect the breccia in many places, hosting the same spectrum of particle types as observed in the surroundings. Thin section show that in contrast to the breccia, phengite crystals are somewhat smaller, ranging between 20 and 30 μm in length. The microstructures suggest crystallization by devitrification of a solidified glass matrix. The breccia clasts within the pseudotachylytes are devoid of any preferred orientation and the lithic fragments are angular.

On outcrop scale the crosscutting pseudotachylyte veins appear completely undistorted. On a microscopic scale there is also no evidence for deformation following pseudotachylyte formation. This implies that the original fabrics of the basal breccia are largely preserved. [Nüchter, 2013]

In literature pseudotachylytes are described to typically form at the brittle-ductile transition within the earth's crust, where rocks are hot enough, but also still brittle enough. At the base of the brittle zone within the earth's crust rocks are already heated to a few hundred degrees and the additional frictional heat caused by an earthquake can lead to melting of the rock. An

earthquake event is very short (seconds) and the molten rock quickly cools again to form a black glass. [Source: Alex Strekeisen

<http://www.alexstrekeisen.it/english/meta/pseudotachylyte.php>]

2.6 General Model

The Preveli subunit underwent folding, metamorphism and exhumation during the Mesozoic, independently from the other subunits of the Uppermost nappes. From the early Cenozoic onwards, the Uppermost units are considered to have been part of the upper crust of the Eurasian active continental margin (Thomson et al., 1998). Owing to the Miocene collision with the Adriatic microcontinent, the upper crust of the active margin (Pelagonian continent) was emplaced on top of the nappe pile that was stacked as a result of the northward directed subduction of the Pindos Ocean. The emplacement of the Preveli nappe on top of the Pindos unit caused, fractures filled with quartz and calcite, cataclastic shear zones, faulting and development of a basal breccia layer. Frictional fusion at seismic strain rates caused the injection of Pseudotachylyte into fractures.

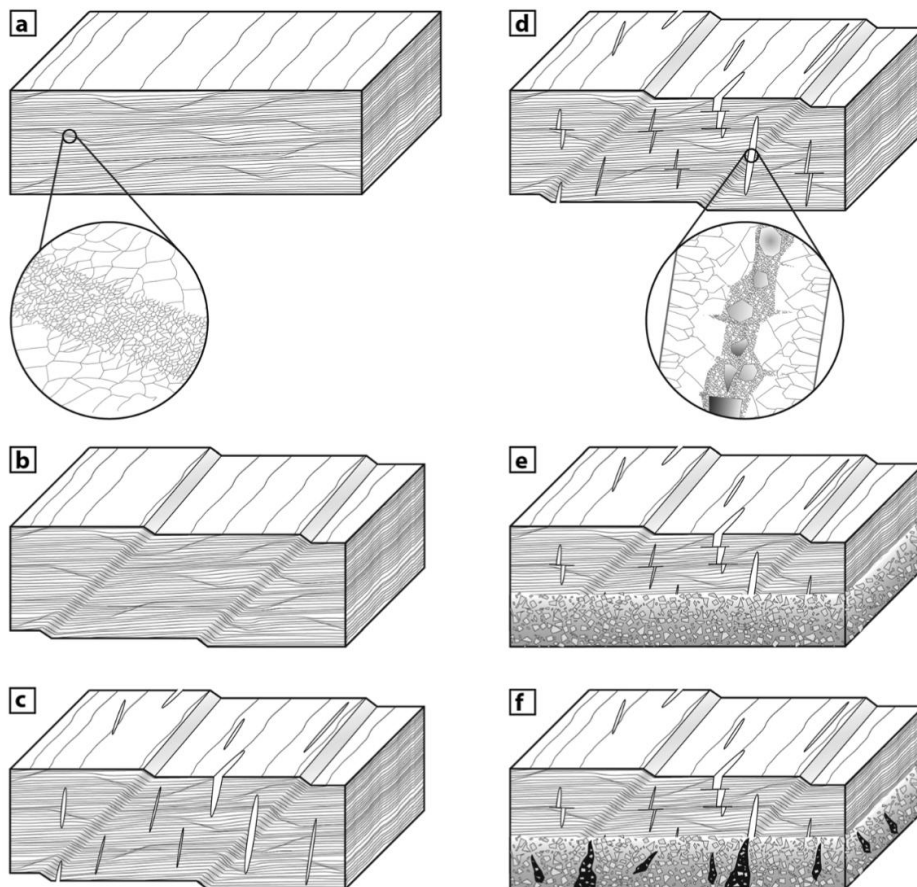
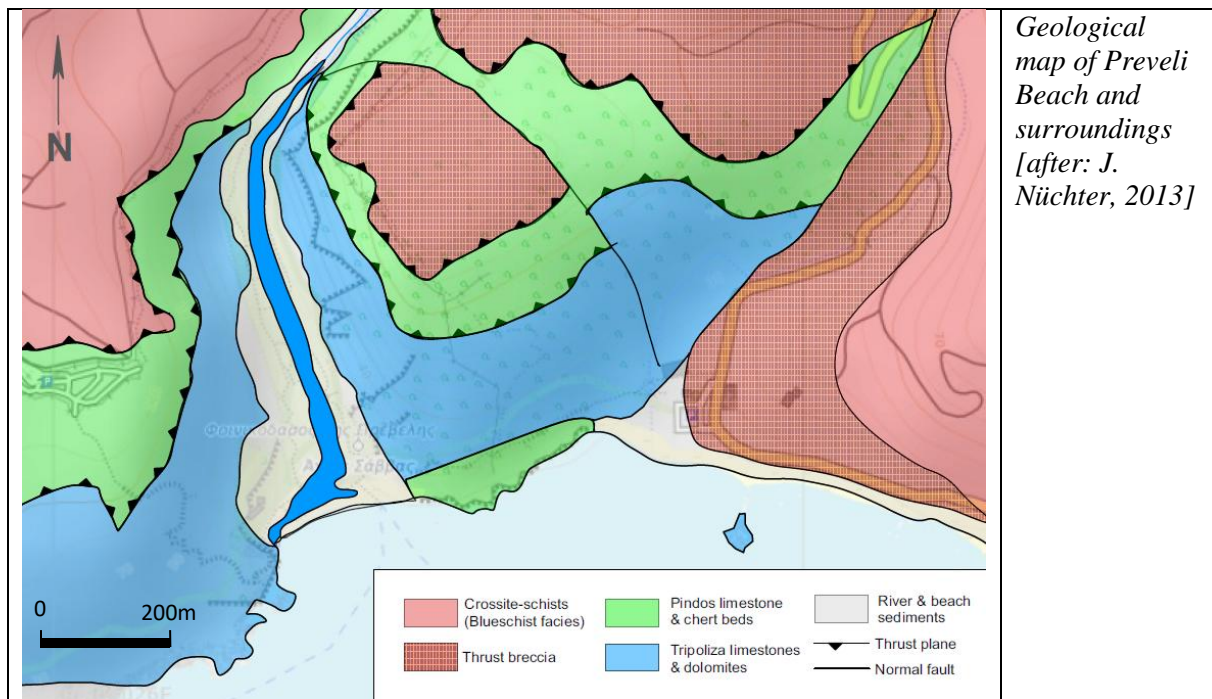


Diagram illustrating the formation of fabrics at the base of the Preveli nappe approximately from the Miocene onwards:

- (a) Small-scale shear zones and crystal-plastic deformation of quartz by dislocation creep.
- (b) Kink bands.
- (c) Tensile failure causing fractures developing to into quartz veins

- (d) Cataclastic shear zones crosscutting the quartz veins and coeval offset of the veins parallel to host rock schistosity.
 (e) Development of the breccia layer by cataclastic deformation at seismic strain rates, culminating into
 (f) frictional fusion and injection of the melt into fractures [Nüchter, 2013]

2.7 The Underlying Pindos Unit and Preveli Beach



Geological map of the area around Preveli beach [after Nüchter 2013]



Outcrop VIII. Pindos Limestone underlying the basal breccia layer. It is largely not metamorphic and bedding is still intact.



View of Preveli beach from the eastern side of the valley rim. In the foreground and at the opposite side of the valley Tripoliza limestone. Preveli beach is well known on Crete owing to its large palm tree grove. A river flows parallel to the beach before entering the sea. Wild geese often spend time at the river bank despite the many bathers.



Location of outcrops. 1: Fault



Outcrop I: Pindos Limestone containing layers of red chert near Preveli beach (eastern steps). The Pindos Unit stratigraphically overlies the Tripoliza limestone. In this case it has been offset by a normal fault and lies below the Tripoliza limestone. The Pindos unit is considered to be a deep marine formation containing micritic limestone and chert, which is often red. The limestone is also sometimes pink.

2.8 Coast Road



Location of outcrops. View of the Mt Korifi and the coast road looking North. [Source Google Maps]



Outcrop I: Metamorphic argillaceous rock; possibly flysch or olistostrome



Outcrop I: Metamorphic argillaceous rock; possibly flysch or olistostrome owing to the light-coloured clasts. 1: argillaceous matrix, 2: clast.



Outcrop II: Dark grey schist (greenstone)



Outcrop II: Limestone/marble (meta-conglomerate?) overlying schist.



Outcrop II: Dark grey schist (greenstone)



Outcrop II: Schist



Outcrop II: Schist. The closeup shows that the former argillaceous rock has numerous fine quartz layers parallel to foliation as well crosscutting quartz veins. Some layers are coarser grained than others.



Outcrop III. Greenschist probably containing chlorite, which gives the rock its green colour.



Outcrop III. Greenschist



Outcrop III. Greenschist. The shiny lustre is due to the presents of mica such as muscovite and/or chlorite orientated along the planes of foliation.

Chlorite is an important rock-forming mineral in low- to medium-grade metamorphic rock formed by metamorphism of mafic or pelitic rock. It is also common in igneous rocks, usually as a secondary

mineral, formed by alteration of mafic minerals such as biotite, hornblende, pyroxene, or garnet. Chlorite is a common weathering product and is widespread in clay and in sedimentary rock containing clay minerals. It is found in pelites along with quartz, albite, sericite, and garnet, and is also found in association with actinolite and epidote. [Wikiwand]



Outcrop III. Greenstones on the beach. The intensive green colour appears to be due to chlorite or epidote.



Outcrop IV, Greenstone, meta-basalt or metagabbro



Outcrop IV, Greenstone, meta-basalt or metagabbro



Outcrop IV, Greenstone, meta-basalt or metagabbro probably containing chlorite



Location of outcrops. View of the south-eastern side of Korifi Mt. displaying green schist and mafic dykes overlain by conglomeratic marble (?). The landslide yields samples from the overlying rock.



Outcrop V. Dark schist with dark vein.



Outcrop V. Close up of previous picture (see box). The large clast (see arrow) appears to have been broken off from the wall of the neighbouring rock either owing to friction during faulting or due to the intrusion of magma or a pseudotachylyte. 1: Magmatic/pseudotachylytic vein, 2: country rock, 3: Clast



Outcrop V. Possible magmatic vein



Outcrop V. Closeup of previous picture: possible magmatic or Pseudotachylyte vein



Outcrop V. Country rock: possibly dark schist



Outcrop VI lies near the steps.



Outcrop VI. Metagabbro or meta-dolerite dyke



Outcrop VI. Metagabbro or meta-dolerite dyke



Outcrop VI. Metagabbro or meta-dolerite dyke



Outcrop VI. Closeup of previous picture. Metagabbro or meta-dolerite dyke



Location of Outcrop VII



Outcrop VII: possible veins containing meta-gabbro or meta-dolerite in dark schist. 1: meta-gabbro or meta-dolerite.



Outcrop VII: closeup of previous picture showing possible meta-dolerite vein



Outcrop VII, closeup: possible meta-dolerite vein

References

- Langosch A. et al., 2000: Intrusive rocks in the ophiolitic melange of Crete ± Witnesses to a Late Cretaceous thermal event of enigmatic geological position, Institut für Mineralogie und Geochemie, Universität zu Köln.
- Tortorici L. et al., 2011: The Cretan ophiolite-bearing mélange (Greece): A remnant of Alpine accretionary wedge, Dipartimento di Scienze Geologiche, University of Catania, C.so Italia
- Cowan D. S. (1985), Structural styles in Mesozoic and Cenozoic mélanges in the western Cordillera of North America, *GSA Bulletin* (1985) 96 (4): 451–462.
- Champod E. et al., 2010: Stampfli Field Course: Tectonostratigraphy and Plate Tectonics of Crete, Université de Lausanne, September 2010
- Zulauf G. et al., 2023: Provenance of far-traveled nappes in the eastern Mediterranean (Uppermost Unit, Crete): constraints from U–Pb zircon ages of detrital and igneous zircons, Institut für Geowissenschaften, Goethe-Universität Frankfurt a.M., Germany
- Martha S., et al., 2018: The tectonometamorphic evolution of the Uppermost Unit south of the Dikti Mountains, Crete, Institut für Geowissenschaften, Goethe-Universität Frankfurt
- Koepke J. and Seidel E., 2004: Hornblendites within ophiolites of Crete, Greece: Evidence for amphibole-rich cumulates derived from an iron-rich tholeiitic melt, Institut für Mineralogie, Universität Hannover, Germany.
- Nüchter J. et al. 2013: Cyclic ductile and brittle deformation related to coseismic thrust fault propagation: Structural record at the base of a basement nappe (Preveli, Crete)
- Thomson S. N. et al., 1989: Apatite fission-track thermochronology of the uppermost tectonic unit of Crete, Implications for the post-Eocene tectonic evolution of the Hellenic Subduction System, Institut für Geologie, Ruhr-Universität Bochum
- Thomson, S. N., Stockert, B. & Brix, M. R. 1999. Miocene high-pressure metamorphic rocks of Crete, Greece: rapid exhumation by buoyant escape. In: Ring, U., Brandon, M. T., Lister, G. S. & Willett, S. D. (eds) *Exhumation Processes: Normal Faulting, Ductile Flow and Erosion*. Geological Society, London, Special Publications, 154, 87-107.
- Chatzaras, v., Xypolias, P. & Doutsos, T (2006): Exhumation of high-pressure rocks under continuous compression: a working hypothesis for the southern Hellenides (central Crete, Greece). - *Geol. Mag.* 143: 859-R76.
- Epting, M., Kudrass, H.-R., Leppig, U. & Schafer, A. (1972): *Geologie der Talea Ori/Kreta*. - *N. Jb. Geol. Palaont. Abh.* 141: 259-285.
- Fassoulas C., Rahl J.M., 2004: Patterns and Conditions of Deformation in the Plattenkalk Nappe, Crete, Greece: A Preliminary Study, Natural History Museum of Crete, Yale University, New Haven, Connecticut
- Hall, R. & Audley-Charles, M.G. (1983): The structure and regional significance of the Talea, Ori, Crete. - *J. Struct. Geol.* 5: 167-179.
- Kull U., 2012: *Kreta, Sammlung geologischer Führer*

Kock S. et al, 2007: Detrital zircon and micropalaeontological ages as new constraints for the lowermost tectonic unit (Talea Ori unit) of Crete, Greece, Geologisch-Paläontologisches Institut der Universität Basel

Krahl, J., Richter, D., Forster, O., Kozur, H. & Hall, R. (1988): Zur Stellung der Talea Ori im Bau des kretischen Deckenstapels (Griechenland). - Z. dtsh. geol. Ges. 139: 191-227.

Manutsoglu, E., Soujon, A., Reitner, J. & Dornsiepen, U.F. (1995a): Relikte lithistider Demospongiae aus der metamorphen Plattenkalk-Serie der Insel Kreta (Griechenland) und ihre palaobathymetrische Bedeutung. - N. Jb. Geol. Palaont. Mh. 1995: 235-247.

Seybold L., 2019: New constraints from U–Pb dating of detrital zircons on the palaeogeographic origin of metasediments in the Talea Ori, central Crete, Ludwig-Maximilians-Universität, Luisenstraße 37, 80333 Munich, Germany

Stampfli 2010: Stampfli Field Course, Tectonostratigraphy and Plate Tectonics of Crete, Université de Lausanne, France

Theye, T, Seidel, E. & Vidal, O. (1992): Carpholite, sudoite and chloritoid in low-grade high-pressure metapelites from Crete and the Peloponnese, Greece. - Europ. J. Mineral. 4 487-507.

Thomson, S.N., Stockhert, B. & Brix, M.R. (1998a): Thennochronology of the high-pressure metamorphic rocks of Crete, Greece: implications for the speed of tectonic processes. - Geology 26: 259-262.

Treppmann, e., Lenze, A. & Stockhert, B. (2010): Static recrystallization of vein quartz pebbles in a high-pressure-low-temperature metamorphic conglomerate. - 1. Struct. Geol. 32: 202-215.

Zulauf G. et al., 2014: Closure of the Paleotethys in the External Hellenides: Constraints from U–Pb ages of magmatic and detrital zircons (Crete), Goethe University, Frankfurt a.M., Germany, University of Patras, GR-26500, Patras, Greece

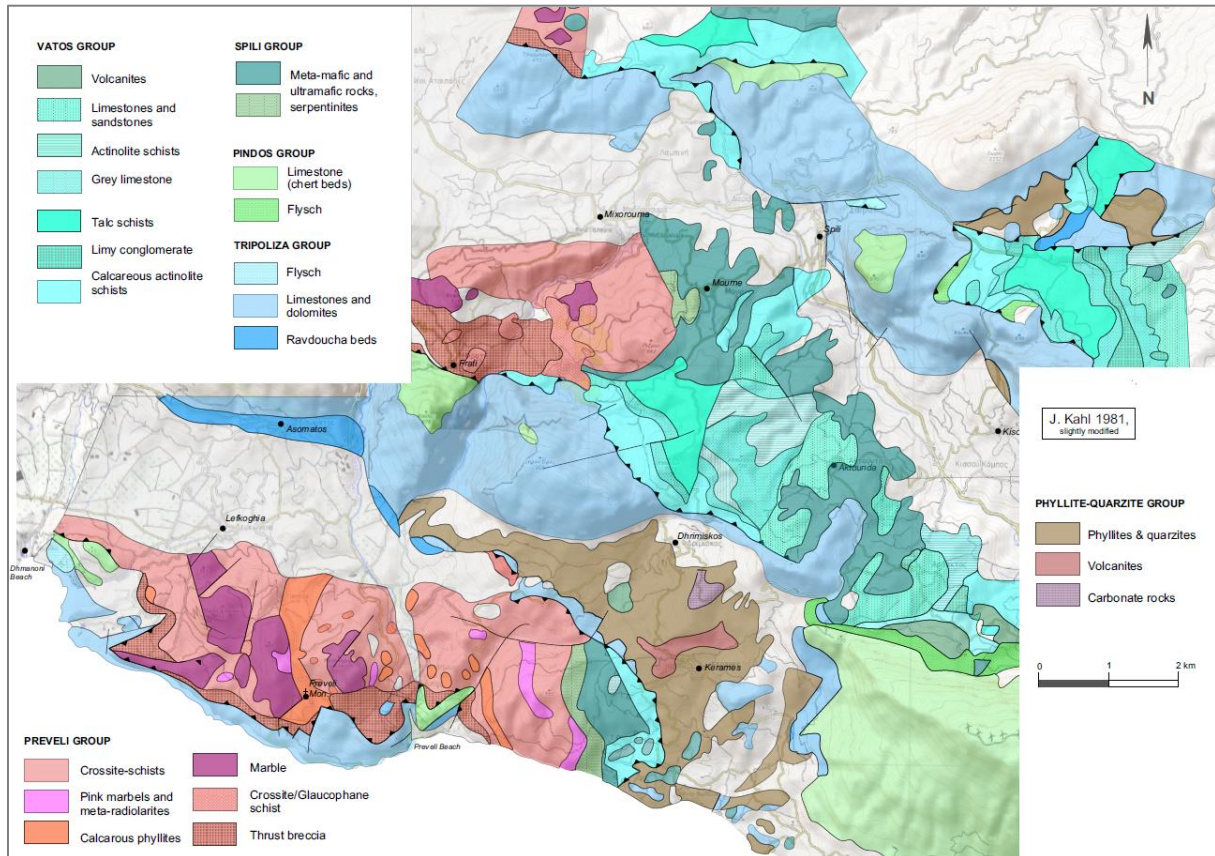
3 Appendix

Geological Time Scale

| Eonothem/ Eon | Erathem/ Era | System/ Period | Series/ Epoch | Stage/ Age | mya ¹ |
|------------------|-----------------|-------------------|------------------|---------------|------------------|
| Phanerozoic | Cenozoic | Neogene | Pliocene | Piacenzian | 2.58 |
| | | | | Zanclean | 3.600 |
| | | | Miocene | Messinian | 5.333 |
| | | | | Tortonian | 7.246 |
| | | | | Serravallian | 11.63 |
| | | | | Langhian | 13.82 |
| | | | | Burdigalian | 15.97 |
| | | | | Aquitanian | 20.44 |
| | | | | | 23.03 |
| | | Paleogene | Oligocene | Chattian | 27.82 |
| | | | | Rupellian | 33.9 |
| | | | | | 37.8 |
| | | | Eocene | Priabonian | 41.2 |
| | | | | Bartonian | 47.8 |
| | | | | Lutetian | 56.0 |
| | | | | Ypresian | 59.2 |
| | | | Paleocene | Thanetian | 61.6 |
| | | | | Selandian | 66.0 |
| | | | | Danian | 72.1 ± 0.2 |
| | Mesozoic | Cretaceous | Upper | Maastrichtian | 83.6 ± 0.2 |
| | | | | Campanian | 86.3 ± 0.5 |
| | | | | Santonian | 89.8 ± 0.3 |
| | | | | Coniacian | 93.9 |
| | | | | Turonian | 100.5 |
| | | | | Cenomanian | 113 |
| | | | Lower | Albian | 125.0 |
| | | | | Aptian | 129.4 |
| | | | | Barremian | 132.9 |
| | | | | Hauterivian | 139.8 |
| | | | | Valanginian | 145.0 |

| Eonothem/ Eon | Erathem/ Era | System/ Period | Series/ Epoch | Stage/ Age | mya ¹ |
|------------------|----------------------------|----------------------------|------------------|---------------|------------------|
| Phanerozoic | Mesozoic | Jurassic | Upper | Tithonian | ~145.0 |
| | | | | Kimmeridgian | 152.1 ± 0.9 |
| | | | | Oxfordian | 157.3 ± 1.0 |
| | | | Middle | Callovian | 163.5 ± 1.0 |
| | | | | Bathonian | 166.1 ± 1.2 |
| | | | | Bajocian | 168.3 ± 1.3 |
| | | | | Aalenian | 170.3 ± 1.4 |
| | | | | | 174.1 ± 1.0 |
| | | | Lower | Toarcian | 182.7 ± 0.7 |
| | | | | Pliensbachian | 190.8 ± 1.0 |
| | | | | Sinemurian | 199.3 ± 0.3 |
| | | | | Hettangian | 201.3 ± 0.2 |
| | Triassic | Upper | Rhaetian | | ~208.5 |
| | | | | Norian | ~227.0 |
| | | | | Carnian | ~237.0 |
| | | Middle | Ladinian | | ~242.0 |
| | | | | Anisian | 247.2 |
| | | Lower | Olenekian | | 251.2 |
| | | | | Induan | 251.902 ± 0.024 |
| | | | | | 254.14 ± 0.7 |
| | Paleozoic | Permian | Lopingian | Changhsingian | 259.1 ± 0.5 |
| | | | | Wuchiapingian | 265.1 ± 0.4 |
| | | | Guadalupian | Capitanian | 268.8 ± 0.5 |
| | | | | Wordian | 272.95 ± 0.11 |
| | | | | Roadian | 283.5 ± 0.6 |
| | | Carboniferous | Cisuralian | Kungurian | 290.1 ± 0.26 |
| | | | | Artinskian | 295.0 ± 0.18 |
| | | | | Sakmarian | 298.9 ± 0.15 |
| | | | | Asselian | 303.7 ± 0.1 |
| | | | | Gzhelian | 307.0 ± 0.1 |
| | | | | Kasimovian | 315.2 ± 0.2 |
| | Mississippian ² | Pennsylvanian ² | Upper | Bashkirian | 323.2 ± 0.4 |
| | | | | | 330.9 ± 0.2 |
| | | | | Serpukhovian | 346.7 ± 0.4 |
| | | Mississippian ² | Middle | Visean | 358.9 ± 0.4 |
| | | | | | |
| | | | | Tournaisian | |

Geological Map of the Uppermost Nappes near Plakias by Krahle, 1981



Geological map of the Uppermost Nappes of south central Crete from Preveli Beach to Spili after Krahle 1981

Plate Tectonic Model for the Uppermost Nappes by Tortorici, 2011

According to Tortorici L. (2011) the Cretan mélangé can be subdivided into three main tectonic units characterized by different metamorphic facies. In Tortorici's plate tectonic model metamorphism took place during one initial event (so called DA-Event). The three main tectonic units each representing a separate nappe are:

1. An un-metamorphosed to weakly metamorphosed lower unit
2. A greenschist to high pressure (HP) greenschist intermediate unit
3. A high pressure/low temperature HP/LT upper unit.

These units show features that associate them with portions of an accretionary wedge [see the Type IV mélangé model presented by Cowan (1985)]. In this context, the lower unit is thus interpreted as a tectonic pile built up at the toe of the accretionary wedge where frontal accretion is dominant. In contrast, the intermediate and upper units represent the innermost and deeper subducted portions of the accretionary wedge, which were exhumed and superimposed on top of each other during the early stages of continent–continent collision. Owing to the existing tectonic features and metamorphic grade, Tortorici, 2011 proposes that, the history of the three units can be described by four different continuous compressional events, which he refers to as the DA–DC and DD events.

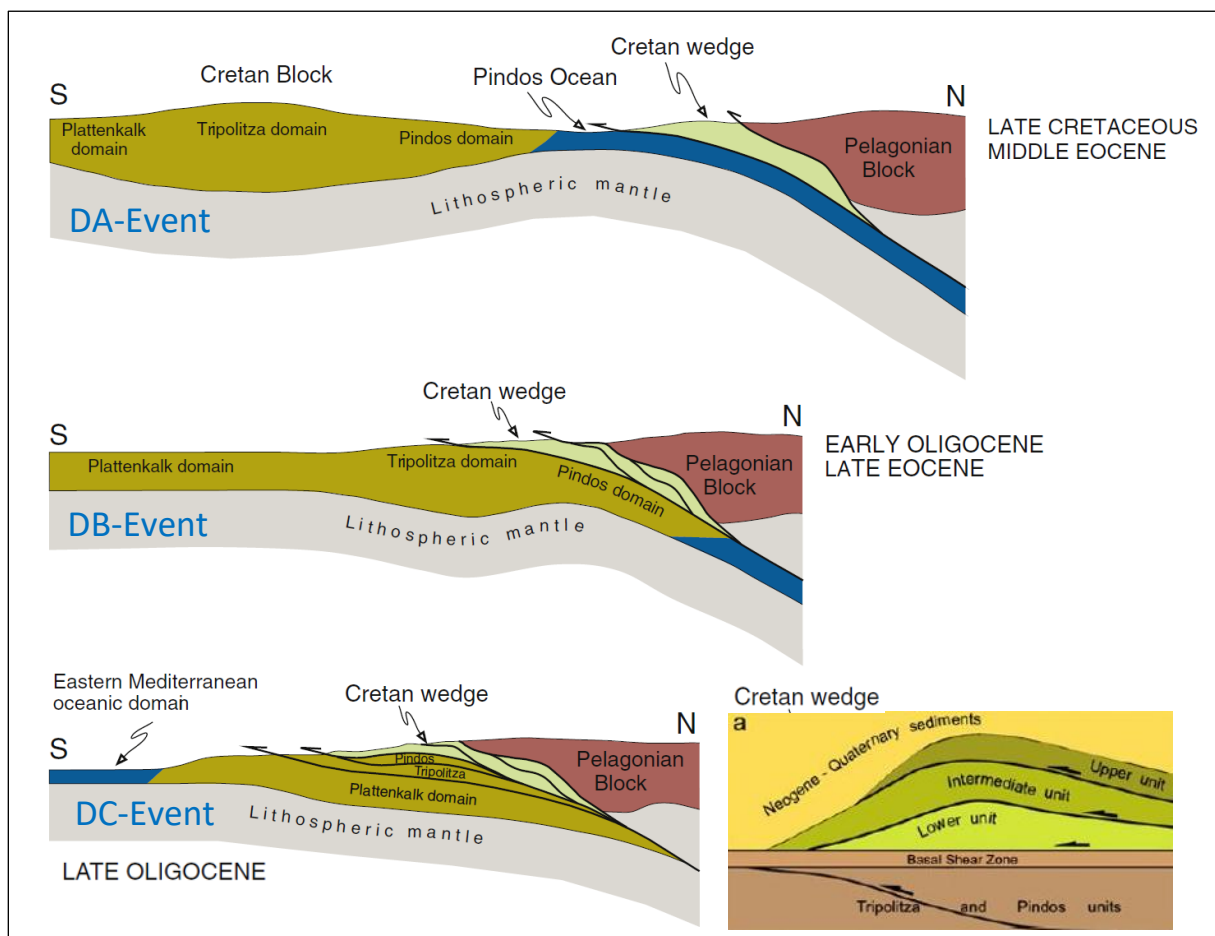


Fig. 14. Schematic drawings (not to scale) illustrating the subduction zone between the Pelagonian (Internal Hellenides Platform continental domains) and the Adria (Cretan) blocks. Tectonic evolution of the Pindos-Cycladic Ocean (cf. Papanikolaou, 2009) and the Cretan accretionary wedge from the Late Cretaceous to the Late Oligocene.

DA Event

The first DA event produced distinct sets of structures that developed at different crustal levels along major shear zones during oceanic subduction. In the un-metamorphosed lower unit the deformation was mostly related to frontal accretion processes at the toe of the accretionary wedge, while in the intermediate and upper units foliation and metamorphism occurred. The structures and metamorphic features of the intermediate and upper units suggest that these tectono-metamorphic units were exposed to greenschist (P-t values of 7–9 kb and 350 °C) and HP/LT (P-t values of 12–14 kb and 350°–450 °C) overprint during subduction. The Early-Middle Eocene greenschist to blueschist facies metamorphism can be related to the under thrusting of the inner portions of the accretionary wedge beneath the Pelagonian continental basement at a depth of about 35–40 km. At this point the total oceanic lithosphere must have been consumed and the onset of the continental collision was taking place.

DB Event

The primary features of the DA Event were subsequently greatly modified by the DB Event that caused the extrusion and uplift of the two intermediate and upper units along the subduction channel during continental collision. The latest stage of the DB Event produced brittle thrusting of the intermediate and upper units onto the un-metamorphosed portions of the wedge. This caused the reverse stacking of the units and imbrication of ophiolite elements. During the Late Eocene–Early Oligocene the exhumation and emplacement of the intermediate and upper units above the frontal portion of the accretionary wedge was mainly due to deep duplexing (Cello and Mazzoli, 1996; Silver et al., 1985). This involved slices of basement-continental rocks being dragged from the backstop where they were incorporated within the deepest portions of the upper unit. Furthermore, larger blocks such as the Asteroussia continental basement rocks were forced into the shallower portions of the extruded wedge (i.e., the intermediate unit) by thrusting of the overriding plate (Ring and Glodny, 2010).

DC Event

The DC event was dominated by the emplacement of the whole Cretan mélange with its three units onto the continental paleomargin of the Cretan Block (also known as the Adria plate). The entire accretionary wedge was thus incorporated in the continental collision and emplaced in the Late Oligocene–Early Miocene above the Cretan continental margin domains (Tripolitza and Pindos domains). Portions of continental paleodomains (i.e. Plattenkalk and Tripolitza basement) were dragged within the subduction zone and successively stacked and exhumed at the leading edge of the upper plate.

DD Event

Finally, the DD event was characterized by thrusting and folding, which took place during the collision of the two continental margins. This involved the south-westward transport of the entire Cretan nappe pile. From the end of the Early Miocene onwards the headlong continent–continent collision produced a large-scale contractional regime that driven by SSW shortening gave rise to the Cretan segment of the External Hellenides.

Conclusions

Tortorici L. (2011) suggests that the ophiolite bearing units of central Crete represent a suture zone between the southeastern edge of the Adria/Cretan Block to the south, and the Pelagonian continental terranes to the north, which evolved from the closure of the Pindos oceanic domain.

Fission track dating

[Wikipedia]



Fission track dating is a radiometric dating technique based on analyses of the damage trails, or tracks, left by fission fragments in certain uranium-bearing minerals and glasses. It is a relatively simple method of radiometric dating that has made a significant impact on understanding the thermal history of continental crust, the timing of volcanic events, and the source and age of different archeological artifacts. The method involves using the number of fission events produced from the spontaneous decay of uranium-238 in common accessory minerals to date the time of rock cooling below closure temperature. Fission tracks are sensitive to heat, and therefore the technique is useful at unraveling the thermal evolution of rocks and minerals. Most current research using fission tracks is aimed at: a) understanding the evolution of mountain belts; b) determining the source or provenance of sediments; c) studying the thermal evolution of basins; d) determining the age of poorly dated strata; and e) dating and provenance determination of archeological artifacts.

Applications

Unlike many other dating techniques, fission-track dating is uniquely suited for determining low-temperature thermal events using common accessory minerals over a very wide geological range (typically 0.1 Ma to 2000 Ma). Apatite, sphene, zircon, micas and volcanic glass typically contain enough uranium to be useful in dating samples of relatively young age (Mesozoic and Cenozoic) and are the materials most useful for this technique. Additionally low-uranium epidotes and garnets may be used for very old samples (Paleozoic to Precambrian). The fission-track dating technique is widely used in understanding the thermal evolution of the upper crust, especially in mountain belts. Fission tracks are preserved in a crystal when the ambient temperature of the rock falls below the annealing temperature. This annealing temperature varies from mineral to mineral and is the basis for determining low-temperature vs. time histories. While the details of closure temperatures are complicated, they are approximately 70 to 110 °C for typical apatite, c. 230 to 250 °C for zircon, and c. 300 °C for titanite.

Because heating of a sample above the annealing temperature causes the fission damage to heal or anneal, the technique is useful for dating the most recent cooling event in the history of the sample. This resetting of the clock can be used to investigate the thermal history of basin sediments, kilometer-scale exhumation caused by tectonism and erosion, low temperature metamorphic events, and geothermal vein formation. The fission track method has also been used to date archaeological sites and artifacts. It was used to confirm the potassium-argon dates for the deposits at Olduvai Gorge. [Wikipedia]



Fission tracks observed in a mineral under optical microscope.

Fission track dating is the method used in thermochronology to find the approximate age of several uranium-rich minerals, such as apatite. When nuclear fission of uranium-238 (^{238}U) happens in inorganic materials, damage tracks are created. These are due to a fast charged particle, released from the decay of Uranium, creating a thin trail of damage along its trajectory through the solid. To better study the fission tracks created, the natural damage tracks are further enlarged by chemical etching so they can be viewed under ordinary optical microscopes. The age of the mineral is then determined by first knowing the spontaneous rate of fission decay, and then measuring the number of tracks accumulated over the mineral's lifetime as well as estimating the amount of Uranium still present. At higher temperatures, fission tracks are known to anneal.

Provenance analysis of detrital grains

A number of datable minerals occur as common detrital grains in sandstones, and if the strata have not been buried too deeply, these minerals grains retain information about the source rock. Fission track analysis of these minerals provides information about the thermal evolution of the source rocks and therefore can be used to understand provenance and the evolution of mountain belts that shed the sediment. This technique of detrital analysis is most commonly applied to zircon because it is very common and robust in the sedimentary system, and in addition it has a relatively high annealing temperature so that in many sedimentary basins the crystals are not reset by later heating.

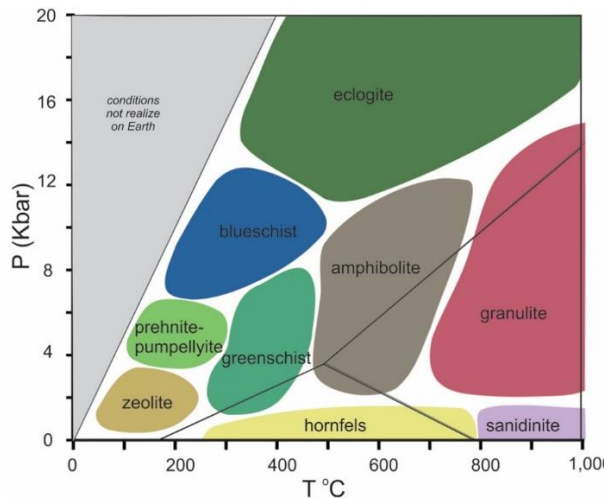
Fission-track dating of detrital zircon is a widely applied analytical tool used to understand the tectonic evolution of source terrains that have left a long and continuous erosional record in adjacent basin strata. Early studies focused on using the cooling ages in detrital zircon from stratigraphic sequences to document the timing and rate of erosion of rocks in adjacent orogenic belts (mountain ranges). A number of recent studies have combined U/Pb and/or Helium dating (U+Th/He) on single crystals to document the specific history of individual crystals. This double-dating approach is an extremely powerful provenance tool because a nearly complete crystal history can be obtained, and therefore researchers can pinpoint specific source areas with distinct geologic histories with relative certainty. Fission-track ages on detrital zircon can be as young as 1 Ma to as old as 2000 Ma. [Wikipedia]

Open Petrology

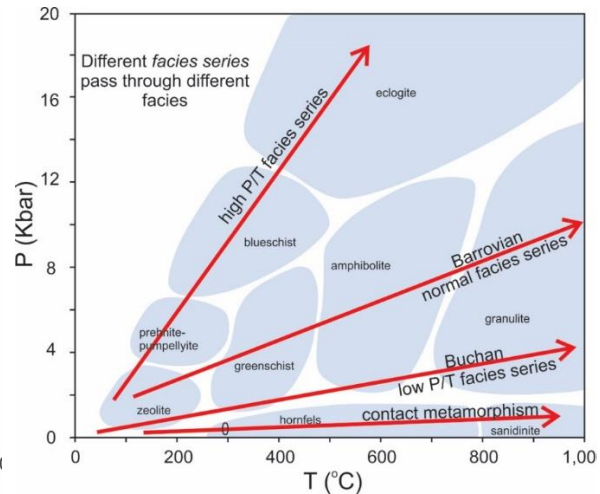
Free Textbook for College-Level Petrology Courses

[Open Petrology – Free Textbook for College-Level Petrology Courses](#)

Metamorphic Facies



8.68 The P-T ranges for different metamorphic facies



8.69 Metamorphic facies series

Zeolite minerals and clays characterize the *zeolite facies*. This facies represents the lowest grade of metamorphism; it is often hard to distinguish zeolite-facies metamorphism from diagenesis. As temperature rises, the zeolite facies gives way to the *prehnite-pumpellyite facies*, the *greenschist facies*, the *amphibolite facies*, and the *granulite facies*. Contact metamorphism produces two low-pressure, high-temperature facies, the *pyroxene-hornfels facies* and the *sanidinite facies*. The *blueschist facies* and the *eclogite facies* occur at high pressure.

Eskola based his facies names on minerals and textures of mafic rocks. The names of the facies are names of different kinds of metamorphosed mafic rocks. But petrologists use the same names when talking about rocks of other compositions. This leads to some confusion. The table below lists key mineral assemblages in mafic rocks, but the assemblages will never be present in rocks of other compositions. For example, pelitic or calcareous rocks do not form greenschists (green mafic schists) or amphibolites (mafic rocks dominated by amphibole and plagioclase) even when metamorphosed at conditions within the greenschist or amphibolite facies. In addition, for some rock compositions, several different mineral assemblages may be stable within a single facies. Further confusion arises because petrologists use some facies names in a more restricted sense, referring to particular rock types with important tectonic significance. Despite these problems, the facies concept provides a convenient way to discuss general ranges of pressure and temperature, and it receives wide use.

| Key Mineral Assemblages in Mafic Rocks of Different Metamorphic Facies | | |
|--|----------------------|--|
| kind of Metamorphism | metamorphic Facies | diagnostic Minerals |
| contact metamorphism | pyroxene hornfels | orthopyroxene + clinopyroxene + plagioclase |
| | sanidinite | sanidine or tridymite or pigeonite or glass |
| low-pressure metamorphism | zeolite | zeolites + quartz |
| | prehnite-pumpellyite | prehnite or pumpellyite + quartz |
| | greenschist | chlorite, epidote, albite, quartz |
| | amphibolite | hornblende + plagioclase |
| | granulite | orthopyroxene or garnet + clinopyroxene + quartz |
| high-pressure metamorphism | blueschist | glaucophane |
| | eclogite | omphacite + garnet ± quartz |

As a model for progressive metamorphism, petrologists consider different *metamorphic facies series*, the sequences of metamorphic rocks that would form in different metamorphic environments. The PT diagram in Figure 8.69 shows the most important of these series.

Rocks undergoing contact metamorphism experience only low pressure. They pass through the zeolite, prehnite-pumpellyite, low-pressure greenschist, pyroxene hornfels and sanidinite facies with increasing temperature. Such rocks are common anywhere magma has intruded shallow crustal rocks.

Rocks subjected to regional metamorphism during mountain building experience a significant increase in both pressure and temperature. They progress through the zeolite, prehnite-pumpellyite, greenschist, amphibolite, and granulite facies. Sometimes they follow a *Buchan facies series* (lower pressure) and sometimes they follow a *Barrovian facies series* (higher pressure).

Subduction carries relatively cool rocks to depth and high pressures. So, some rocks related to subduction zones follow the *high P/T facies series*, experiencing conditions in the zeolite, prehnite – pumpellyite, blueschist, and possibly eclogite facies. We find these rocks, typically, as blocks in fault contact with greenschist facies rocks. Petrologists have described blueschists from many places, but the two classic examples of the blueschist facies series are rocks of the Sanbagawa metamorphic belt of Japan and of the Franciscan Complex of California.

Metamorphosed Pelitic Rocks (Metapelites)

Slate

Slates, which form during low-grade metamorphism of shales, comprise primarily microscopic clay grains, perhaps with some minor mica. Metamorphism may obliterate the original bedding as foliation develops perpendicular to the direction of maximum stress. This foliation, *slaty cleavage*, gives slates a property called *fissility* – an ability to break into thin sheets of rock with flat smooth surfaces. The minerals in these rocks cannot be identified in hand specimen, but in thin section quartz, feldspar, and chlorite can be seen. Slates come in many colors, but various shades of gray are most common. Thin sheets of slate have historically been used for paving or roofing stone.

Phyllite

Figure 8.27 shows a sample of phyllite, a shiny foliated rock created by further metamorphism of slates. The foliation is due to parallel alignment of very small – mostly microscopic – muscovite, chlorite, or other micas, sometimes with graphite. Phyllites, which form at higher metamorphic grades than slates, sparkle because clay minerals have metamorphosed to produce small grains of reflective mica. Thus, foliation of phyllites is different from the foliation in slates that stems from clay mineral alignment, and different from foliation in schists because schists always contain visible mica grains. Like slates, phyllites exhibit fissility.



8.27 Example of a phyllite



8.28 muscovite schist

Phyllites are typically black, gray, or green, and the fine-grained micas and graphite, which are too small to see without a microscope, give phyllites their silky/shiny appearance, or sheen, called a phyllitic luster. It is this luster – which is absent from slate and schist – that really defines a phyllite. Additionally, although not seen in Figure 8.27, layering in some phyllites is deformed, giving the rocks a sort of wavy or crinkly appearance.

Schist

Schists, which form under medium-grade metamorphic conditions, contain medium-to-coarse flakes of aligned mica that we can easily see. This photo (Figure 8.28) shows a typical schist. Schists are higher-grade rocks than phyllites, and most form when phyllites are further metamorphosed. Thus, the precursors of schist are shale, slate, and phyllite. Less commonly, however, schist may form by metamorphism of fine-grained igneous rocks, such as tuff or basalt. Large and aligned flaky minerals, easily seen with the naked eye, define schists. These minerals are most commonly muscovite (such as in this photo) or biotite in parallel or near-parallel orientations that give the rocks schistosity – the ability to be broken easily in one direction but not in other directions.

Most schists are mica schists, but graphite, talc, chlorite, and hornblende schists are common. Quartz and feldspar are present in mica schists, often deformed or elongated parallel to the micas, and many other minerals are possible. If schists contain prominent minerals, we name them accordingly. So the schist in Figure 8.23 is a garnet schist, and the one in Figure 8.28 is a muscovite schist, or simply a mica schist.

Metapelites derive from the metamorphism of shale and other clay-rich sediments. When metamorphosed, dehydration reactions change clay minerals into new minerals containing less H₂O. At low grade this leads to the formation of chlorite and muscovite. At higher grade, biotite forms. Foliated textures develop as muscovite and biotite crystallize, so metapelites may be slates, phyllites, schists or gneisses depending on grade.

Gneiss

At higher grades, metamorphic rocks may develop compositional layering because different minerals concentrate in layers of contrasting colors. We call such rocks *gneisses*. The defining characteristics of most gneisses, such as the gneisses seen in Figure 8.29 and Figure 8.31, are that the rocks are medium- to coarse-grained and contain alternating layers of light and dark-colored minerals that give the rock foliation called *gneissic banding*.



8.29 A biotite-quartz gneiss. The specimen is 6.8 cm across



8.31 Deformed granitic gneiss

Gneisses, the highest temperature-pressure kinds of foliated metamorphic rock, typify many regions that have undergone high-temperature metamorphism. Gneissic banding most commonly forms in response to directed stress. Sometimes, however, layering may form solely due to chemical processes that concentrate different minerals in different layers. The felsic light-colored layers typically contain quartz and feldspars, and the more mafic darker layers typically contain biotite, hornblende, or pyroxene. Accessory minerals such as garnet are common. Sometimes gneissic banding is deformed, as seen in Figure 8.31. This gneiss, from the Czech Republic, contains pink K-feldspar rich layers alternating with darker layers that contain biotite. Metamorphism produced parallel layers of contrasting mineralogy (and color) and subsequent deformation caused the layers to become deformed.

Gneisses are often named based on their protoliths, and petrologists use the general terms *orthogneiss* for gneisses derived from igneous rocks, and *paragneiss* for gneisses derived from sedimentary rocks. More specific names abound – for example, *pelitic gneisses* form by metamorphism of originally clay-rich sedimentary rocks, *granitic gneisses* (such as the one shown in Figure 8.31) form by metamorphism of granites, and *mafic gneisses* form by metamorphism of mafic igneous rocks. Sometimes key minerals are often included in rock names. For example, a *garnet gneiss* is a gneiss that contains conspicuous garnet crystals.

Some gneisses do not display well-defined dark- and light-colored banding but still maintain less distinct foliation. For example, the foliation in kyanite gneiss may come from alignment of light-colored kyanite crystals in an otherwise quartz- and muscovite-rich rock. An *augen gneiss*, contains large feldspar crystals – “eyes” (*augen* is German for eyes) – stretched in one direction.

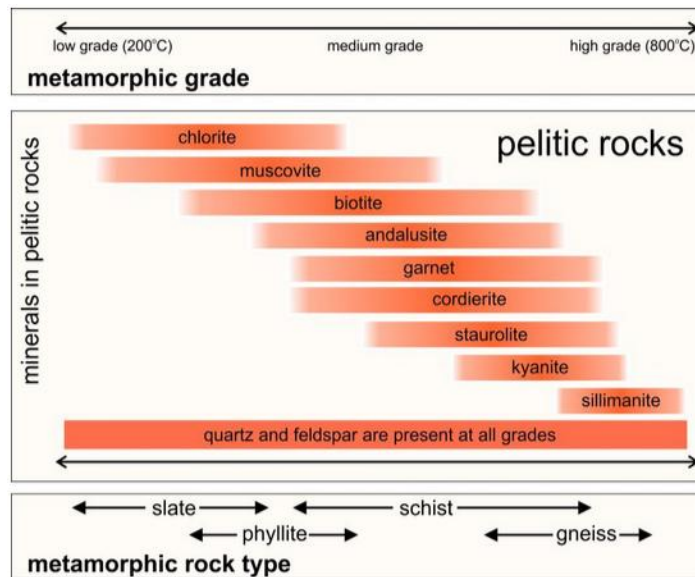
Minerals in Metapelites

Metapelites are rich in Al, Si, and K and may contain substantial amounts of Fe and Mg, so minerals containing these elements dominate metapelitic rocks. The table below lists the most common and important minerals in these rocks. The minerals in the left column may exist in low-grade rocks, those in the right column are exclusively in high-grade rocks, and the ones in the middle are generally in medium-grade rocks.

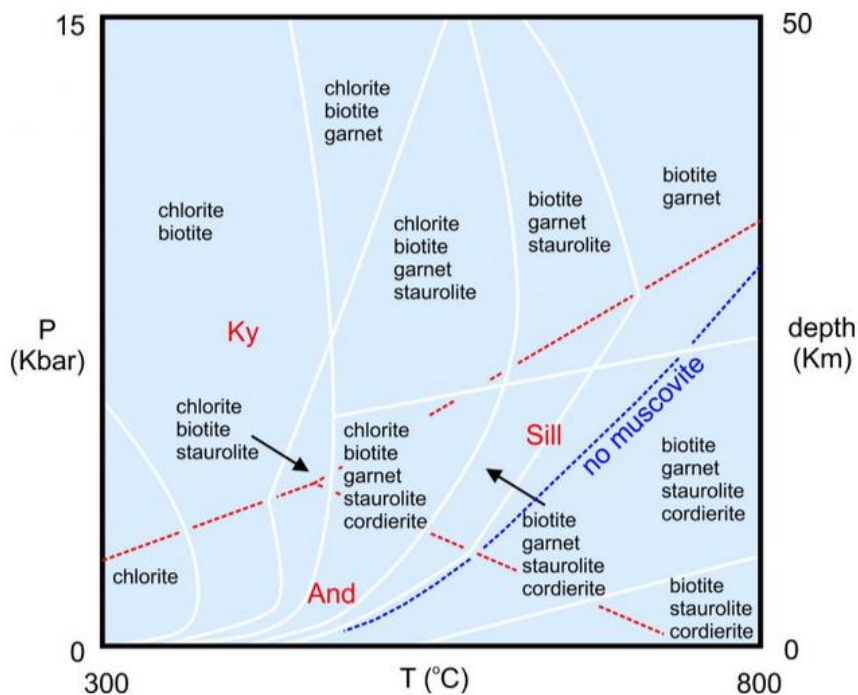
| Common Minerals in Metapelites | | |
|--|---|--|
| low grade | → | high grade |
| quartz SiO_2 | muscovite $\text{KAl}_2(\text{AlSi}_3\text{O}_{10})(\text{OH})_2$ | staurolite $(\text{Fe,Mg})_2\text{Al}_9\text{Si}_4\text{O}_{23}(\text{OH})$ |
| kaolinite $\text{Al}_4(\text{Si}_4\text{O}_{10})(\text{OH})_8$ | kyanite Al_2SiO_5 | cordierite $(\text{Mg,Fe})\text{Al}_4\text{Si}_5\text{O}_{18}$ |
| pyrophyllite $\text{Al}_2(\text{Si}_4\text{O}_{10})(\text{OH})_2$ | andalusite Al_2SiO_5 | K-feldspar KAlSi_3O_8 |
| chlorite (variable chemistry) | biotite $\text{K}(\text{Mg,Fe})_3(\text{AlSi}_3\text{O}_{10})(\text{OH})_2$ | sillimanite Al_2SiO_5 |
| chloritoid $(\text{Fe,Mg})_2\text{Al}_4\text{Si}_2\text{O}_{10}(\text{OH})_4$ | garnet (almandine) $(\text{Ca,Fe,Mg,Mn})_3\text{Al}_2\text{Si}_3\text{O}_{12}$ | orthopyroxene $(\text{Mg,Fe})_2\text{Si}_2\text{O}_6$ |

The chart in Figure 8.42 shows typical minerals in metapelites at different grades. Quartz and Na-rich plagioclase are in rocks of all grades. Kaolinite, pyrophyllite and chloritoid may also be present at low grade but are less common and are omitted from this figure. There is a great deal of overlap and many of these minerals exist together. Some persist over a wide range of temperatures. Some are present in low-pressure rocks but not in high-pressure rocks. Either muscovite or biotite are generally present except at the highest grades.

Figure 8.48 shows pressure-temperature stability fields for common pelitic mineral assemblages. Besides the minerals listed, quartz and plagioclase are present under all conditions. The bounding white lines are really diffuse boundaries and the reactions that relate one assemblage to another are complex.



8.42 Minerals as indicators of metamorphic grade in metapelites



8.48 Stable mineral assemblages in metapelites

Many metapelitic rocks contain an Al_2SiO_5 polymorph (andalusite, kyanite, or sillimanite) besides the mineral listed. Red lines and text in this phase diagram show the stability fields for the different polymorphs: kyanite at high pressure, sillimanite at high temperature, and andalusite at low pressure. At medium- or high-grade, Barrovian metamorphism often yields rocks containing kyanite or sillimanite with garnet. At lower pressures, Buchan metamorphism may produce rocks with andalusite, and often cordierite instead of garnet. Muscovite is generally absent at the highest temperatures because it dehydrates to K-feldspar, sillimanite, and water vapor (at temperatures above the blue dashed line).

Metamorphosed Limestones and Dolostones (Marbles)

Geologists generally call metamorphosed carbonate rocks *marbles*, although this term is used in different ways by building contractors and others. The metamorphism of limestone or dolostone composed only of carbonate minerals produces few mineralogical changes. A general increase in grain size may take place – similar to what happens when sandstone turns into quartzite, but no diagnostic minerals can form because of the limited chemical composition and the high stabilities of both calcite and dolomite. The photo in Figure 8.52 shows a marble that contains only coarse crystals of white calcite. Figure [8.36](#), earlier in this chapter, showed a marble consisting only of blue calcite.

However, most limestones contain some quartz and other minerals besides carbonates. In these rocks, a series of interesting Ca-silicates, Ca-Mg-silicates, and Ca-Al-silicates form as metamorphism progresses. The table below lists the most important of these minerals, roughly in order of their appearance in response to increasing metamorphic grade.

| Minerals Common in Metacarbonates | | |
|---|--|--|
| low grade | → | high grade |
| calcite CaCO_3 | talc $\text{Mg}_3\text{Si}_4\text{O}_{10}(\text{OH})_2$ | grossular (garnet) $\text{Ca}_3\text{Al}_2\text{Si}_3\text{O}_{12}$ |
| dolomite $\text{CaMg}(\text{CO}_3)_2$ | tremolite $\text{Ca}_2\text{Mg}_5\text{Si}_8\text{O}_{22}(\text{OH})_2$ | periclase MgO |
| quartz SiO_2 | forsterite $(\text{Mg,Fe})_2\text{SiO}_4$ | wollastonite CaSiO_3 |
| phlogopite (Mg-rich biotite) $\text{K}(\text{Mg,Fe})_3(\text{AlSi}_3\text{O}_{10})(\text{OH})_2$ | diopside $\text{CaMgSi}_2\text{O}_6$ | monticellite CaMgSiO_4 |

If quartz is present, the metamorphic reactions in marbles are often decarbonation reactions that involve the breakdown of carbonates to release CO_2 . If a pluton intrudes a limestone or dolostone, contact metamorphism may cause CO_2 to flow out of the carbonate and combine with H_2O that comes from the pluton. The CO_2 - H_2O fluid can have profound effects on the carbonate nearby, and fluid composition controls the formation of many minerals. Fluids may also cause significant metasomatism and a significant change in rock chemistry.

Phlogopite is typically one of the first minerals to form during carbonate metamorphism. The first photo in the block above (Figure 8.53) shows large, somewhat hexagonal, flakes of phlogopite with calcite behind. The second photo (Figure 8.54) shows gray blades of tremolite in a marble that also contains small (hard to see) specs of graphite.



8.53 *Phlogopite in marble from Orange County, New York*



8.54 *Tremolite and graphite in marble from Franklin, New Jersey*

Metamorphosed Mafic Rocks (Metabasites)

Metamorphosed basalts and other rocks of similar composition are commonly called *metabasites*. This is because, geologists once called basalts *basic rocks*. Compared with metasandstones and metapelites, metabasites are relatively poor in Al and Si and rich in Ca, Mg, and Fe. Many different minerals may form, and metamorphic reactions are complex. Plagioclase and augite are stable at all grades but other minerals are not. The most important metamorphic minerals are Ca and Mg silicates. Metabasites are generally more massive and less foliated than pelitic rocks, but at higher grades they do form schist and gneiss. The table seen below lists the most common minerals in metabasites. Low-grade minerals are at the top of the table, and grade increases downward. Metamorphism often begins with the formation of zeolites, or of prehnite. These minerals may crystallize in vugs or cracks. They are secondary minerals in many igneous rocks, and form by hydration of feldspars when water flows through the protolith. Some petrologists do not consider these minerals to be metamorphic minerals, while others do.

The formation of greenstones is said by many to be the beginning of metamorphism. *Greenstones* are fine-grained, very low-grade metabasites that have a conspicuous light- to dark-gray or green color. The characteristic green color comes from fine-grained chlorite and epidote in the rocks. Greenstones may also contain Na-rich plagioclase (albite), quartz, carbonates, and zeolites.

At slightly higher grades, metabasites become greenschists, obtaining schistosity from parallel arrangements of the green amphibole actinolite and chlorite. Figure 8.66, below, shows a greenschist from the Homestake Gold Mine in Lead, South Dakota. Although hard to see, the specimen contains native gold near the bottom of the sample.

At still higher grade, chlorite, epidote, and actinolite break down by dehydration reactions, producing a specific kind of rock called an *amphibolite*. The photo in Figure 8.67 is an example. Amphibolites contain large grains of black hornblende and whitish plagioclase in subequal proportions. Garnet, biotite, and light-colored amphiboles such as anthophyllite or cummingtonite may also be present. With even more metamorphism, mafic rocks may become mafic gneisses. At the highest grades, all amphiboles become unstable and dehydrate to produce pyroxenes. Assemblages including garnet and clinopyroxene, or orthopyroxene, are diagnostic of mafic granulites.



8.65 Greenstone from Ely, Greenstone Belt, Minnesota



8.66 Greenschist from the Homestake Mine, South Dakota



8.67 Amphibolite from the Geopark Prague, Czech Republic

| Common Minerals in Metabasites | | |
|--------------------------------|---|--|
| | minerals | rock names |
| low grade | zeolites (variable Ca-Al silicates) | |
| | prehnite $\text{Ca}_2\text{Al}(\text{AlSi}_3\text{O}_{10})(\text{OH})_2$ | igneous rock with secondary minerals |
| | pumpellyite (similar to epidote) | |
| | Ca-rich plagioclase $(\text{Ca},\text{Na})_2(\text{Si},\text{Al})_4\text{O}_8$ | |
| | epidote $\text{Ca}_2(\text{Al},\text{Fe})_3(\text{Si}_3\text{O}_{12})(\text{OH})$ | |
| | chlorite (variable chemistry) | greenstone |
| | actinolite $\text{Ca}_2(\text{Fe},\text{Mg})_5(\text{Si}_8\text{O}_{22})(\text{OH})_2$ | |
| | hornblende (complex amphibole) | amphibolite |
| | garnet (almandine-pyrope) $(\text{Fe},\text{Mg})_3\text{Al}_2\text{Si}_3\text{O}_{12}$ | mafic gneiss |
| | biotite $\text{K}(\text{Mg},\text{Fe})_3(\text{AlSi}_3\text{O}_{10})(\text{OH})_2$ | |
| high grade | augite (pyroxene) $\text{CaMgSi}_2\text{O}_6$ | mafic granulite |
| | orthopyroxene (enstatite) $\text{Mg}_2\text{Si}_2\text{O}_6$ | |

High-Pressure Rocks and Minerals

Because of their tectonic significance, petrologists group high-pressure metamorphic rocks into a class unrelated to rock composition. These rocks include mainly blueschists and eclogites, both quite rare. They come from deep in Earth, and special conditions are required to create them and bring them to Earth's surface. Blueschist is a name given to one type of rock that forms at conditions within the blueschist facies, a facies characterized by high pressure and relatively low temperature. Blueschist chemistry is variable. Compositions range from pelitic to mafic. No matter their compositions, they contain conspicuous mineralogy.

A blue amphibole, called glaucophane, is responsible for the name of the facies. The blueschist seen below in Figure 8.78 is mostly glaucophane. Other common blueschist minerals include a colorless to green Na-pyroxene called jadeite, green or white lawsonite, and pale aragonite (the high-pressure polymorph of calcite). Epidote, garnet, zoisite, quartz, and other accessory minerals may also be present. Because they form at low temperature, blueschists are often fine grained, poorly crystallized, and difficult to study.

Eclogites, such as the one seen below in Figure 8.79, are mafic rocks metamorphosed at high pressure and moderate-to-high temperature. They contain the essential minerals pyrope (Mg-rich garnet) and the green Na-rich clinopyroxene called omphacite. Orthopyroxene may also be present in significant quantities. Accessory minerals include kyanite, quartz, spinel, titanite, and many others. Eclogites originate in the deep crust or in the mantle. Many mantle xenoliths, carried up as nodules within magma, are eclogites. Eclogites are also found as layers or bands associated with some peridotites. Quite commonly, eclogites undergo retrograde metamorphism and so become partially changed into blueschists.

| in Metamorphosed High-Pressure Rocks | |
|--------------------------------------|--|
| | minerals |
| low grade | glaucophane $\text{Na}_2(\text{Fe,Mg})_3\text{Al}_2\text{Si}_8\text{O}_{22}(\text{OH})_2$ |
| | lawsonite $\text{CaAl}_2\text{Si}_2\text{O}_7(\text{OH})_2 \cdot \text{H}_2\text{O}$ |
| | epidote $\text{Ca}_2(\text{Al}_2\text{Fe})_3\text{Si}_3\text{O}_{12}(\text{OH})$ |
| | jadeite $\text{NaAlSi}_2\text{O}_6$ |
| | aragonite CaCO_3 |
| | kyanite Al_2SiO_5 |
| | garnet (pyrope-almandine) $(\text{Mg,Fe})_3\text{Al}_2\text{Si}_3\text{O}_{12}$ |
| high grade | omphacite $(\text{Ca,Na})(\text{Mg,Fe,Al})\text{Si}_2\text{O}_6$ |

The photos below show some additional examples of high-pressure minerals. The light-colored crystals in Figure 8.80 are *lawsonite*. Lawsonite has about the same composition as anorthite. But plagioclase (including anorthite and albite components) becomes unstable at high pressure, so the anorthite part hydrates and we get lawsonite instead. The green *jadeite*, in Figure 8.81, is an Na-rich pyroxene that is only stable at high pressure. It forms because the albite component in plagioclase changes by solid-solid reaction into Na-pyroxene. *Glaucophane*, the inky blue mineral in the lower left photo (Figure 8.82) is an Na-rich amphibole. Like omphacite, it incorporates its sodium component from albite. In this specimen, a silvery and greenish chrome mica, *fuchsite*, accompanies the glaucophane. The green omphacite in the lower right photo (Figure 8.83) is a pyroxene that includes a few high-pressure components. And the pyrope (red garnet) in the same sample formed by solid-solid reactions involving pyroxenes.



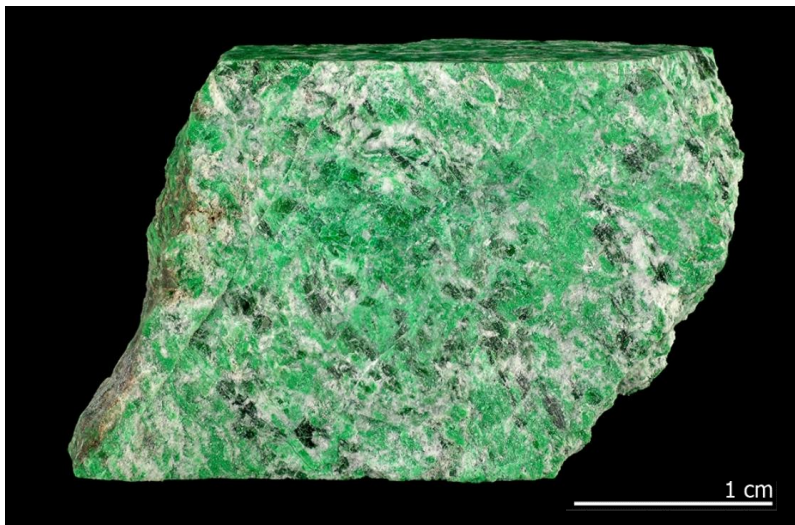
8.78 Blueschist from Marin County, California. 4.7 cm across.



8.79 Eclogite from Almenning, Norway. About 7.5 cm across



8.80 *Lawsonite crystals from Marin County, California. The specimen is 5.5 cm across*



8.81 *Emerald green jadeite from Myanmar*



8.83 *Green omphacite and red pyrope from Nordfjord, Norway. The specimen is 10 cm across*